Studying Protein-DNA Interactions Using Kinetic Capillary Electrophoresis

Alexander Petrov

A DISSERTATION SUBMITTED TO THE FACULTY OF GRADUATE STUDIES

IN PARTIAL FULFILMENT OF THE REQUIREMENTS

FOR THE DEGREE OF

DOCTOR OF PHILOSOPHY

GRADUATE PROGRAM IN BIOLOGY

YORK UNIVERSITY,

TORONTO, ONTARIO

December 2012

Abstract

Protein-DNA interactions are essential to a cell as they control all vital cellular functions such as DNA replication, repair, recombination and transcription. In order to understand the dynamics of these fundamental biological processes, it is important to know kinetic parameters for all steps involved in the formation and dissociation of relevant DNA-protein complexes. We propose Kinetic Capillary Electrophoresis (KCE) as a conceptual platform for development of kinetic homogenous affinity methods for measuring kinetic parameters of such interactions. KCE is defined as the capillary electrophoresis (CE) separation of species that interact during electrophoresis. All KCE methods are described by the same mathematics: the same system of partial differential equations with only initial and boundary conditions being different. One of the advantages of KCE is that mathematical modeling is not necessary for some of them. Here, I i) present the theoretical bases of KCE and propose a multi-method KCE toolbox as an integrated kinetic technique, ii) develop a new KCE method with simplified mathematical approach, iii) introduce a predictive mixing parameter that is essential for diffusion-based mixing in general and to KCE in particular, iv) demonstrate the advantage of the proposed concept for studying complex protein-DNA interactions. Being based on CE separation, KCE is a powerful tool for testing different hypotheses of interactions and accurately calculating multiple binding parameters such as i) high-affinity (specific) and low-affinity (non-specific) interactions that occur within the same protein-DNA pair ii) disassembly of DNA-multiple proteins complexes. The concept of KCE allows for the creation of an expanding toolset of powerful kinetic homogeneous affinity methods, which will find their applications in studies of biomolecular interactions, quantitative analyses, and selecting affinity probes and drug candidates from complex mixtures.

Dedicated to:

my parents

Thank you for your love and support

Acknowledgements

I would like to thank my supervisor Dr. Sergey Krylov for his guidance, patience and support throughout all these years. The frequent discussions about experiments, plans and problems helped me a lot. He taught me how to develop scientific ideas into good research papers.

I would also like to thank the mathematicians that I worked with: Dr. Victor Okhonin and Dr. Leonid Cherney for their help in my research. They taught me a lot about the usefulness of mathematical approach to experimental problems.

Many thanks to the Krylov lab members for their critical input, helpful suggestions, problem discussions and company.

Special thanks to my committee members Dr. John McDermott and Dr. Katalin Hudak for the time they spend to serve as my committee members, their critical evaluation of my work, suggestions and supervision.

Finally I would like to thank York University and NSERC for their financial support of my studies.

Table of Contents

List of Tables

List of Figures

Commonly Used Abbreviations

3D: three dimentional 5

CE: Capillary Electrophoresis 13

cNECEEM: continuous NECEEM 20

CZE: Capillary Zone Electrophoresis 14

DNA: Deoxyribonucleic acid ii

dsDNA: double-stranded DNA 60

E. Coli: *Escherichia coli* 9

EMSA: Electrophoretic Mobility Shift Assay 6

EOF: Electroosmotic Flow 14

FRET: Förster resonance energy transfer 9

FTIR: Fourier Transform Infrared Spectroscopy 4

HPLC: High Pressure Liquid Chromatography 59

KCE: Kinetic Capillary Electrophoresis ii

K_d: equilibrium dissociation constant 3

k_{off}: rate dissociation constant 3

k_{on}: rate association constant 3

MS: Mass Spectrometry 4

NECEEM: Non-Equilibrium Capillary Electrophoresis of Equilibrium Mixtures 15

NMR: Nuclear Magnetic Resonance 4

nt: nucleotide 78

ppKCE: plug-plug KCE 20

QO: Quantitative Overlap 51

RNA: Ribonucleic acid 2

RU: Resonance or Response Units	10
SPR: Surface Plasmon Resonance	4
SSB protein: Single-Stranded Binding protein	1
ssDNA: single stranded DNA	1
sSweepCE: short SweepCE	20
sSweepCEEM: short SweepCE of Equilibrium Mixtures	20
SweepCE: Sweeping Capillary Electrophoresis	15
TDLFP: Transverse Diffusion of Laminar Flow Profiles	49
ZMW: Zero-Mode Waveguide	12

Chapter 1. Introduction

The presented material was published previously. Parts of the text and figures with and without modifications were taken from the following article:
Berezovski, M.; Okhonin, V.; **Petrov, A.**; S.N. Krylov. Kinetic methods in capillary electrophoresis and their applications. *Proc SPIE-Int Soc Opt Eng* **2005**, *5969*, 203-215.

Contribution to the article: performed SSB-DNA KCE experiment, NECEEM aptamer selection experiments.

1.1 Biological Importance of Protein-DNA Interactions

DNA in one of the molecules that are vital for a cell, as it contains all the necessary information to facilitate cell growth, differentiation, housekeeping activities and ultimately cell death. However, by itself the DNA is just a storage of information, which needs to be decoded and maintained in order to be useful. For that, DNA depends on non-covalent affinity interactions with other molecules present in a cell, such as proteins. Proteins participate in such vital processes as: DNA replication, repair, recombination and transcription, but in order to perform these tasks, proteins must interact with DNA. These interactions can be specific when a protein binds to the defined sequence and non-specific when a protein can bind to any site available on the DNA.[1]

An example of proteins exhibiting non-specific protein-DNA interactions is the family of Single-Stranded Binding (SSB) proteins. They bind to single stranded DNA (ssDNA) regions that arise during normal cellular activities, such as replication and transcription. SSB proteins' functions include stabilization of ssDNA regions as well as preventing undesired reactions with the exposed DNA region.[2] Additionally, SSB proteins can recruit partner proteins and initiate their binding to ssDNA[3-5] as well as stimulate their biochemical activities[6-8].

An example of proteins that interact with DNA in a specific manner is a broad group of proteins called transcription factors. A transcription factor is a protein that binds the specific DNA sequence located upstream of the translation initiation site and regulates gene transcription.[9] This regulation can occur through interactions with either RNA polymerase itself or with other transcription factors. A transcription factor can either repress or activate transcription of a certain gene.[10] To activate transcription a transcription factor may, upon binding, promote assembly of a transcriptional complex[10-12] or induce a conformational change in an already bound complex stimulating the activity and/or stability[10, 13, 14]. To repress transcription, a transcription factor may bind to a regulatory element preventing the activating transcription factor from binding to a DNA element[10, 15, 16] or by binding to the activating transcription factor directly and inhibiting its ability to stimulate transcription[10, 17, 18].

It is clear that the interplay between proteins and DNA, that involves both protein-DNA and protein-protein non-covalent interactions, is fundamental to biology. A prime example is the discovery in 2006 of four transcription factors that could transform adult differentiated skin cells into pluripotent stem cells,[19] that enabled use of induced stem cells instead of embryonic stem cells. While use of novel genome-wide methods such as next generation sequencing combined with chromatin immunoprecipitation have demonstrated the importance of protein-DNA interactions,[20] they provide only the part of the story. While the identified proteins and their respective DNA sequences form a molecular basis for a biological model, there is still much speculation about the mechanism of interactions between them. The detailed *in vitro* studies are required to test proposed models and confirm the role that protein-protein and protein-DNA

interactions are playing in regulation of replication, repair, recombination and transcription processes.

To do that, one needs to study affinity interactions between the protein of interest and the corresponding DNA sequence. The simplest affinity interaction between DNA and a protein (P) can be described by the following equation:

$$P + DNA \underset{k_{off}}{\overset{k_{on}}{\rightleftharpoons}} P \bullet DNA \qquad 1.1$$

where k_{on} is rate association constant, k_{off} is rate dissociation constant, while the affinity of a protein to DNA can be defined by equilibrium dissociation constant, $K_d = k_{off}/k_{on}$. Although K_d is a useful parameter for determining whether an interaction is likely to take place, K_d alone provides no information on the dynamics of interactions. For example, a decrease in K_d could be caused by a protein binding more readily to a DNA element (k_{on} increases) or when a protein-DNA complex is stabilized and dissociates more slowly (k_{off} decreases), two very different scenarios. Similarly, an increase in K_d may represent a protein not binding as readily (k_{on} decreases) or more rapid dissociation (k_{off} increases). The changes in kinetic parameters are typically caused by a protein interacting with other proteins, DNAs or small molecules. Thus, the kinetics of interactions provide invaluable information for determining the mechanisms that underlie processes such as cooperative binding of proteins to DNA, allosteric regulation and steric hindrance.

1.2 Methods for Analysis of Protein-DNA Interactions

1.2.1 General Classification

Methods for measurement of equilibrium and rate constants can be classified into two categories: mixture-based and separation-based (see **Figure 1.1**). The first category includes light absorption, fluorescence spectroscopy, Nuclear Magnetic Resonance (NMR), Fourier Transform Infrared spectroscopy (FTIR), Mass Spectrometry (MS), Raman spectroscopy, potentiometry, calorimetry and Surface Plasmon Resonance (SPR). The separation-based methods include dialysis, ultrafiltration, ultracentrifugation, chromatography (liquid chromatography and thin-layer chromatography) and electrophoresis (planar and capillary electrophoresis). Separation-based methods can detect individual interacting components and/or complexes, thus avoiding the interference of other components. Though some conventional methods, such as dialysis, ultrafiltration, ultracentrifugation, chromatography, and planar electrophoresis, are widely used to study interactions, they are constrained by a number of factors, such as Donnan effect, nonspecific adsorption, leakage of bound molecules through membrane, excessive analysis time, large sample size, as well as errors due to sedimentation and viscosity.

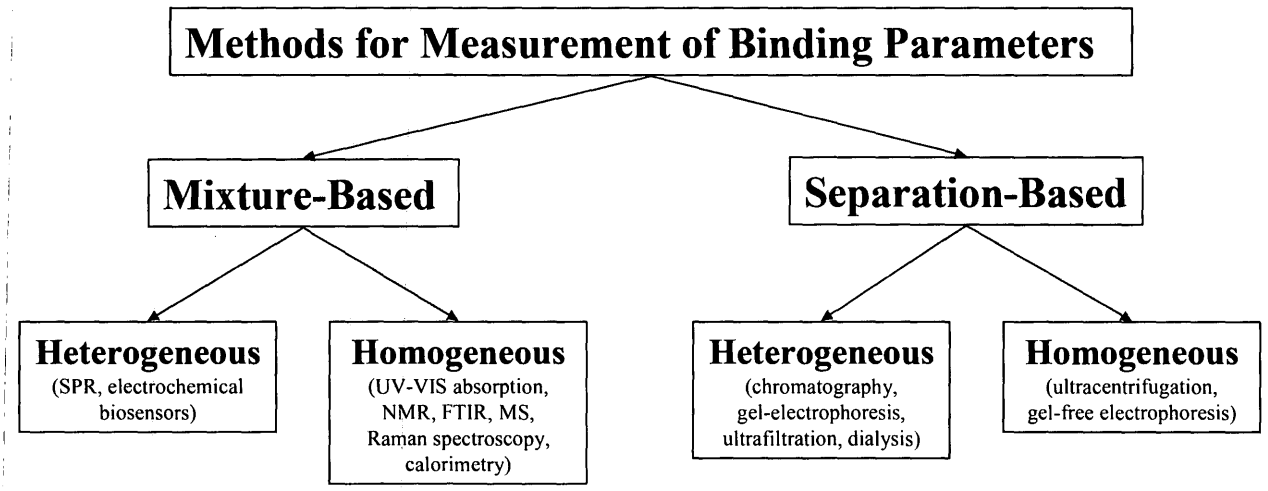

Figure 1.1 Methods for measurement of binding parameters

Mixture-based and separation-based methods can be subdivided into two broad categories: heterogeneous and homogeneous binding assays. In heterogeneous assays, one of the components is affixed to a solid substrate, while the other one is dissolved in a solution and can bind the component affixed to the surface.

Heterogeneous binding assays have certain advantages and drawbacks. The most serious drawback is that affixing a molecule to the surface may change the 3-dimentional (3D) structure. The extent of such change will depend on the method of immobilization, and can potentially affect binding. In addition, the immobilization on a surface may be time-consuming and expensive, and non-specific interactions with the surface are always a concern.

In homogeneous binding assays, components are mixed and allowed to form a complex in solution; neither of the molecules are affixed to the surface. Complex formation is followed by monitoring the changing physical-chemical properties of components upon binding. Such properties can be optical (absorption, fluorescence, polarization) or separation-related (chromatographic or electrophoretic mobility).

As previously mentioned, it is desirable to obtain not only the equilibrium constants for protein-DNA interactions, but also the kinetic constants. A brief review of kinetic-capable methods along with their respective advantages and limitations is given below.

1.2.2 Electrophoretic Mobility Shift Assay

The first classical method for measuring the affinity of a protein binding to DNA is Electrophoretic Mobility Shift Assay (EMSA), introduced back in 1981.[21] In this method the equilibrium mixture of protein and DNA is subjected to non-denaturing gel electrophoresis. The individual components of the equilibrium mixture are then separated based on the size to charge ratio. As the complex typically has a smaller net negative charge than DNA and is bulkier, it produces more friction with the gel matrix, and migrates through the gel slower than DNA, creating a "shift" of a DNA band compared to the DNA-only control as shown in **Figure 1.2**.[22]

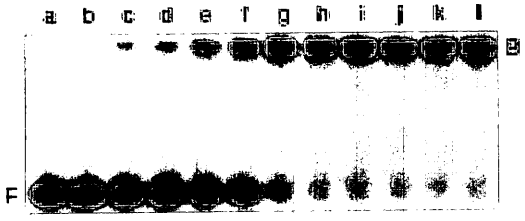

Figure 1.2 Titration of a 16-residue single-stranded DNA with human AGT protein. As the protein concentration increases more and more DNA shifts from free (F) fraction to bound (B) fraction. Adopted from Hellman *et al*, 2007

The DNA of interest can be labelled and after the separation the bands that correspond to DNA and protein-DNA complex are quantitated using radioactive, fluorescent or chemiluminescent detection modes.[22] Alternatively, components can be visualized by silver staining[23] after the electrophoresis. As the amounts of protein-DNA complex, unbound DNA and stoichiometry of interactions can be deduced from the number of bands and their intensity, the K_d values can be calculated.

This method is applicable to a wide range of proteins from relatively small peptides to transcription complexes and is compatible with both purified proteins and cell lysates.[24] A wide range of nucleic acid sizes can be used from several nucleotides to several thousands of nucleotides of either single or double-stranded nucleic acids.[24] EMSA can also be used for determination of stoichiometry of interactions.[25] The method is very robust, easy to perform and works under a wide range of binding conditions.

Theoretically, the method is capable of directly measuring not only equilibrium constants, but also dissociation rate constants of protein-DNA interactions. To do that, the area between the bands of complex and free DNA should be quantified and knowing the separation time, the half-life of a complex could be estimated. Practically, however, it is not feasible as there are a number of limitations.

The major limitation of the EMSA technique is that complexes tend to be more stable in a gel than in a free solution.[26] The major factor in stabilizing the interactions is likely the volume exclusion effect of the gel matrix.[27, 28] In some cases, the separation between the dissociated DNA and the protein does not occur fast enough to prevent rebinding. Thus, multiple association/dissociation events may occur during the separation, making analysis of dissociation kinetics a non-trivial task. The same effect can lead to an error in estimation of k_{on} in time-progression studies, where the amount of complex is determined at different time points.

Despite the limitations listed above, that make the method semi-quantitative and suitable only for measuring equilibrium constants, it is still widely used due to its simplicity and low cost of necessary equipment and consumables.

1.2.3 Stopped-Flow Technique

An alternative method to study kinetics of interactions is the stopped-flow method. The stopped flow method was first introduced by Chance in 1940.[29] A typical instrumental setup is shown in **Figure 1.3** and consists of several syringes, depending on the number of species to be mixed, a mixer and a flow stopper. Conceptually, the technique is very simple, the solutions containing molecules of interest are rapidly mixed in a specific mixing chamber by a high speed flow. Once mixed, the mixture is rapidly introduced into an observation chamber and the flow is abruptly stopped. The mixing is fast and the dead time between the mixing and the start of monitoring is typically on the millisecond scale.[30] The stopped-flow instrument can be interfaced with a number of different detectors: absorbance, fluorescence, conductivity, calorimetry, circular dichroism and light scattering.[31, 32] The data is presented as a change in optical signal *vs.* time. The resulting kinetic curve can be fitted and both k_{on} and k_{off} constants can be determined. The method can also be used to determine the effect of the extrinsic factors, such as temperature or pH, on the interaction kinetics.[31]

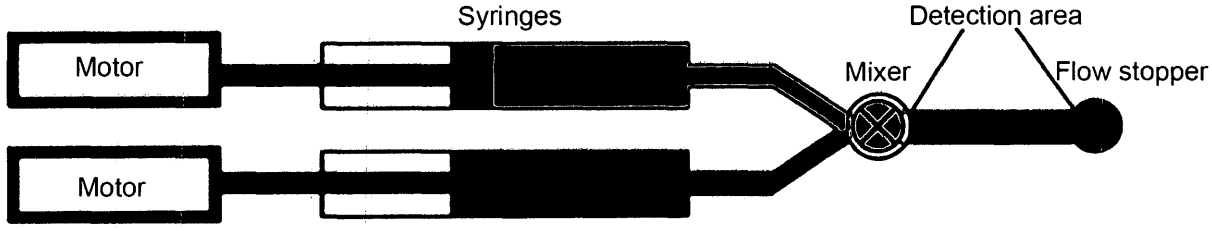

Figure 1.3 Diagram of a stopped-flow instrument

The advantage of this technique is that since the dead time between the initiation of the reaction by mixing and observation is on the millisecond level, the reactions with fast k_{on} can be studied. Andreeva *et al.*[33] used the stopped flow method combined with anisotropy detection to study the interactions between the Rep A helicase and DNA. The study showed that the reaction

occurred through the four-step sequential mechanism with the protein-DNA complex undergoing multiple conformational transitions.[33] A similar study was done by Fedorova *et al.*[34] for the enzymatic reaction between *E. Coli* Fpg protein and corresponding DNA substrate containing oxidized DNA residues. Using stopped-flow technique and monitoring the change in intrinsic fluorescence the authors were able to see four discrete stages that comprised the binding and enzymatic steps of the reaction and determine the rate constants for each step.[34]

One of the major limitations of the stopped flow technique is the requirement that a reaction between molecules of interest should produce a detectable difference in optical signal, which is not always the case.[31] This can be improved by using fluorescence quenching or Förster resonance energy transfer (FRET) probes, but it requires some *a priori* information about 3D structure to design a probe the fluorescent intensity of which would change. The most significant drawback is that there is no separation between interacting molecules and therefore association/dissociation reactions that occur simultaneously will give rise to a single kinetic curve, which described a combination of multiple kinetic processes. Additional complications, such as high experimental noise or unknown number of reacting species, make it impossible to deconvolute the individual kinetic parameters from such a curve.[35]

1.2.4 Surface Plasmon Resonance

The most comprehensive method that can measure kinetic constants is SPR. The SPR method is based on the physical phenomenon of partial light absorption that occurs, when a light beam of polarized light shines on a metal film at a certain incidence angle. The angle at which the maximum adsorption of light occurs is called the SPR angle. The SPR angle is dependent on refractive indices on both sides of a metal, thus if a protein is in proximity of a gold surface the

refractive index would change and so would the SPR angle. So by monitoring changes in the SPR angle, it is possible to monitor kinetics of protein binding to the surface or molecules immobilized on the surface.[36] A change in the SPR angle is described in terms of Resonance or Response Units (RU), the plot of signal in RU over time is called a sensorgram.

The gold surface of an SPR chip is essential for plasmon resonance phenomenon, but is not well suited for the biomolecular interactions, thus the surface is typically covered with a polymer matrix. The matrix provides a hydrophilic environment suitable for interaction studies, serves as an anchor for the attachment of molecules to the surface and increases a surface capacity by adding a third dimension.[36]

To study interaction kinetics, one of the molecules of interest, typically DNA, is immobilized in a matrix. A buffer that contains a protein of interest is introduced into an SPR detection cell as shown in **Figure 1.4, left**.[37] Once in proximity of immobilized DNA, a protein can bind to it. This changes the refractive index and respectively the SPR angle. This corresponds to the association part of a sensorgram schematically depicted in **Figure 1.4, right**.[37] Once the steady state is reached, the wash with plain buffer containing no protein commences. This disrupts the equilibrium and the dissociation of the protein bound to DNA begins, giving the dissociation part of a sensorgram. By fitting the resulting graph, both k_{on} and k_{off} rate constants can be determined.

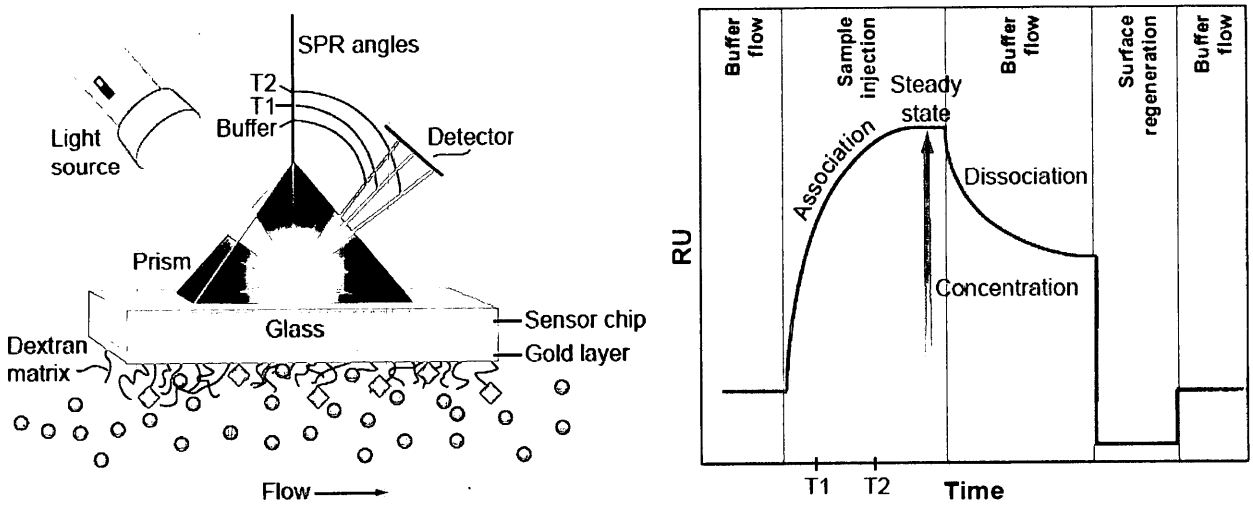

Figure 1.4 General concept of SPR. On the left is a schematic depiction of SPR detection cell. The green spheres binding to red diamonds immobilized on the gold surface producing the change in SPR angle. As the time progresses the angle shifts from blue (buffer control) to red T1 and then T2. The corresponding sensorgram is shown on the right. Adopted from Wilson, 2002

SPR is a popular method and is frequently used for kinetic studies of protein-DNA interactions[38-40] as the commercial instrumentation and developed methodologies for such studies are readily available.

The method has several drawbacks such as the requirement for DNA immobilization on a chip. While the chemistry for DNA immobilization is relatively simple and straightforward, special care should be taken with the amount of the immobilized DNA. If density of DNA would be too high, the rate of protein binding to the immobilized DNA could exceed the rate at which it is delivered with the flow. In such a case, the measured value for the k_{on} constant would be lower than the true value.[41] Similarly, during the dissociation phase, the dissociated protein could rebind before completely diffusing out of a matrix and being washed away by a buffer flow. Thus, the obtained k_{off} value would be smaller than the real value.[41] The method cannot accurately measure fast k_{on} rates that approach 10^6 M^{-1} s^{-1} (the actual upper limit depends on the size of a protein).[41]

The major problem, however, is the lack of separation between the reacting molecules of interest. An SPR instrument would register any binding event that causes a change in the refractive index and is not able to discriminate between specific and non-specific protein-DNA interactions. For that purpose, a minimal DNA fragment is used for binding studies to minimise the non-specific interactions that may occur.[42] Similarly, multiple association/dissociation reactions occurring on the surface of a chip would generate a single kinetic curve that is composed of a sum of several exponential curves. In many cases, such a cumulative curve cannot be used to reliably determine the individual rate constants.[35]

1.2.5 Single-Molecule Spectroscopy

Recent advances in nanofabrication allowed for creation of nanophotonic confinement structures such as Zero-Mode Waveguides (ZMWs). A ZMW is essentially a circular well of 50-200 nm diameter formed by a metal film deposited on a solid, transparent substrate.[43] Use of ZMWs allows observation of volumes in the zeptoliter range, reducing the background signal and allowing observation of reactions between a single molecule that is immobilized on a surface and other molecules that are present in a well.

ZMWs have been used to observe the binding of individual transfer RNAs to the translating ribosome.[44] Another study by Tsai *et al.*[45] studied possible pathways in the formation of ribosomal preinitiation complex. By using ZMWs, it is possible to monitor the binding of individual molecules, which makes it a powerful tool for studying heterogeneous biological pathways.[45]

One of the limitations of the method is that multiple experiments are required in order to calculate rate association/dissociation constants, since rate constants are statistical parameters

that involve statistically significant number of binding/dissociation events. This method is relatively new and there are no commercial instruments available, thus the methodology is not readily transferable between labs and the use of such devices requires significant background knowledge of photonics. The method requires individual labelling of reacting molecules, in such a way, that the attached label does not affect biochemical properties of the molecule of interest, which may not be always possible.

1.2.6 Conclusions

While methods for studying protein-DNA interactions do exist, there are only two comprehensive methods for kinetic studies and each has a number of important limitations. The described methods either require complex labeling of reacting components and/or immobilization on a surface. To address these limitations and increase the number of methods that are available to researchers in the field of protein-DNA interactions, we decided to develop our approach based on separation in Capillary Electrophoresis (CE).

1.3 Introduction to Capillary Electrophoresis

CE is a family of analytical techniques that separate molecules of interest in a small bore glass tube. Conceptually, a typical CE instrument consists of a capillary with both ends immersed in buffer reservoirs and a high voltage power supply as shown in **Figure 1.5**. The sample can be introduced into a capillary by inserting the inlet end of a capillary into a vial containing a sample and applying either a pressure pulse or voltage potential. CE can be interfaced with a variety of detectors including: fluorescence, absorbance, conductivity, electrochemical and mass spectrometry. Depending on the separation mode, molecules of interest can be separated based on differences in: molecular weight, size-to-charge ratio, isoelectric point and hydrophobicity.

One of the CE separation modes that can be used for studies of protein-DNA interactions is Capillary Zone Electrophoresis (CZE). It is the simplest form of CE, where separation of molecules occurs due to differences in their size-to-charge ratios in the absence of any matrix and in a homogeneous buffer solution. One of the phenomena that accompanies CZE is the Electroosmotic Flow (EOF). EOF is the movement of buffer cations that are attracted to the negatively charged silanol groups on the inner surface of a glass capillary, which is exposed to a buffer solution. Once an electric field is applied to a capillary, cations start to move in the direction of the negatively charged electrode dragging the bulk of solution with them, as shown in **Figure 1.5**. The presence of EOF allows one to analyse molecules regardless of their charge, assuming that the EOF speed is fast enough to overcome the mobility of the negatively charged molecules in the opposite direction. The unwanted effect of EOF may be that the molecules of interest are eluted before separation between them is achieved, making accurate quantification impossible.

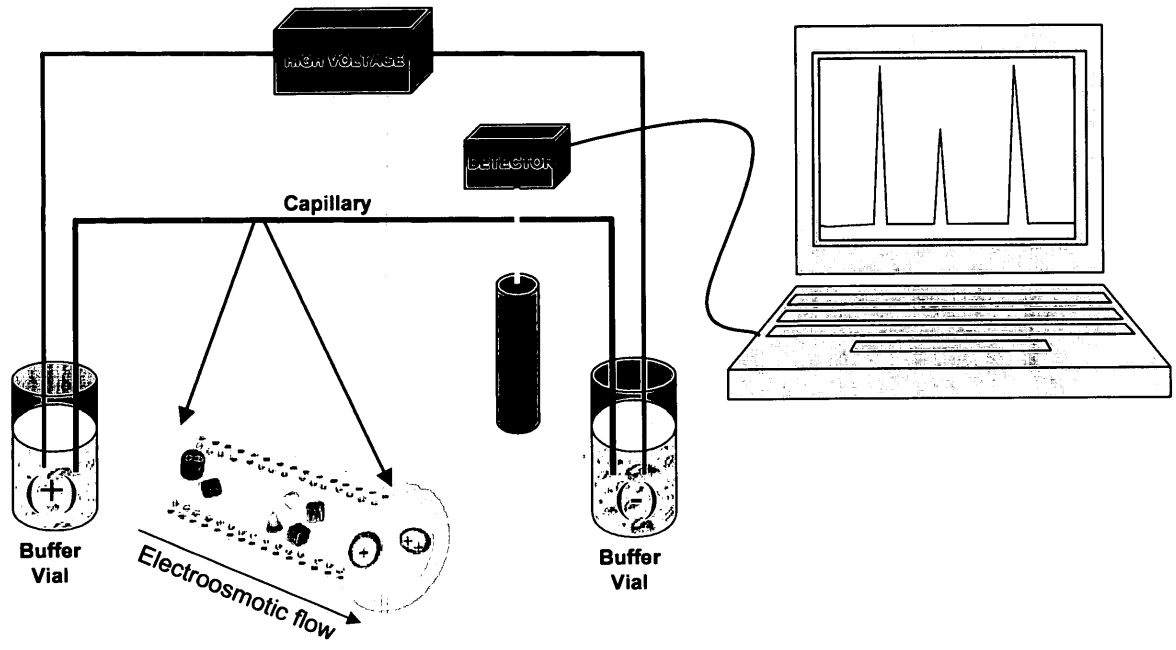

Figure 1.5 Diagram of a CE system

CE methods have a number of advantages. The heat dissipation is very efficient as the ratio between the volume and the surface area of a capillary is very small. This allows the application of electric fields of up to 1000 V/cm, resulting in fast and efficient separation. As a capillary diameter is on a micrometer scale, the sample consumption is equally small, and is typically on a nanoliter scale, which is important for proteins and ligand libraries that are not available in high volumes. The commercial availability of robotic instruments, allows for automation of analysis and decrease the cost and human error factor.

1.3.1 Existing Capillary Electrophoresis Methods

Despite the potential of CE there was little effort to use CE for kinetic studies of protein-DNA interactions prior to introduction of two kinetic CE methods: Non-Equilibrium Capillary Electrophoresis of Equilibrium Mixtures (NECEEM)[46] and Sweeping Capillary Electrophoresis (SweepCE).[47] All prior CE methods assumed equilibrium conditions during the separation with a single exception by Whiteside *et al*[48], and, as a result of such assumption it is impossible to find

rate constants of observed interactions. NECEEM was the first method that allowed to find both K_d and k_{off} from a single experimental graph.[46] In turn, SweepCE was the first non-stopped-flow method that allowed direct measurements of k_{on} constant from a single experiment.[47]

The goal of this dissertation was to unify the existing KCE methods by developing a single conceptual platform. Such platform would simplify the design of new kinetic methods for studies of protein-DNA interactions, and would be tailored to suit the experimenter's needs, depending on which parameters one would with to study. To achieve this we introduced a concept that we call Kinetic Capillary Electrophoresis.

Chapter 2. Kinetic Capillary Electrophoresis

The presented material was published previously. Adapted with permission from **Petrov, A.**; Okhonin, V.; Berezovski, M.; Krylov, S. N., Kinetic capillary electrophoresis (KCE): a conceptual platform for kinetic homogeneous affinity methods. *J Am Chem Soc* **2005,** *127* (48), 17104-10.

Contribution to the article: performed all KCE experiments, participated in data analysis, prepared figures, participated in manuscript writing.

2.1 Introduction

Affinity methods play a crucial role in modern life sciences. In addition to affinity purification, their applications include: quantitative analyses of biomolecules,[49] studies of biomolecular interactions,[50] and selection of affinity probes and drug candidates from complex mixtures, such as combinatorial libraries[51]. Conceptually, all affinity methods are based on non-covalent binding of a Ligand (L) and a Target (T) with the formation of a ligand-target Complex (C):

$$L + T \underset{k_{off}}{\overset{k_{on}}{\rightleftharpoons}} C \qquad 2.1$$

where k_{on} and k_{off} are rate constants of complex formation and dissociation, respectively. The stability of C is typically described in terms of the equilibrium dissociation constant, $K_d = k_{off}/k_{on}$.

This work is concerned with separation-based affinity methods, which are based on the physical separation of free L from C. Depending on how separation is carried out, these methods can be classified as heterogeneous or homogeneous. In heterogeneous methods,[52] T is affixed to a solid substrate, while L is dissolved in a solution. The complexes are formed on the surface while free L remains in solution, thus allowing for separation of L from C. Heterogeneous methods often suffer from non-specific binding of L to the surface and changes in the affinity

caused by the immobilization of T.[53] In homogeneous methods, both T and L are dissolved and the complexes are formed in a solution.[54] Separation of L from C is then achieved based on differences in the mobility of L and C in the homogeneous phase (e.g. by electrophoresis).

Separation-based affinity methods can also be classified as kinetic or non-kinetic. Kinetic methods are those that do not assume equilibrium in reaction 2.1 and can thus be used for: (i) quantitative affinity analyses with "weak" affinity probes (high k_{off}), (ii) measuring k_{on} and k_{off}, and (iii) selection of binding ligands with pre-determined k_{on} and k_{off}. Non-kinetic methods, in contrast, assume equilibrium and, thus, cannot serve for these tasks. The assumption of equilibrium in non-kinetic methods is not conceptually required; moreover, equilibrium cannot be maintained in separation-based affinity methods. Thus, all non-kinetic methods can be converted to kinetic methods by changing conditions and approaches for data analysis.

In general, homogeneous methods are preferable due to their simplicity and kinetic methods are preferable due to their enabling kinetic features. Until recently, the only method with comprehensive kinetic capabilities was SPR, a heterogeneous method.[37] We introduced the first two separation-based homogeneous methods with comprehensive kinetic capabilities: Non-Equilibrium Capillary Electrophoresis of Equilibrium Mixtures (NECEEM),[46] and Sweeping Capillary Electrophoresis SweepCE [47]. The spectrum of their applications already includes: (i) measuring k_{on}, K_d, and k_{off},[46, 47, 55-57] (ii) quantitative affinity analyses of proteins,[56-58] (iii) measuring temperature inside the capillary,[59] (iv) studying thermochemistry of affinity interactions,[60] and (v) kinetic selection of ligands from combinatorial libraries.[61] This work was inspired by the insight that NECEEM and SweepCE are based on the same conceptual platform,

which we call Kinetic Capillary Electrophoresis (KCE). It was further driven by the idea that the concept of KCE can be used to design new kinetic homogeneous affinity methods.

2.2 Theoretical Bases of KCE

We define KCE as CE separation of species, which interact during electrophoresis. Thus, KCE involves two major processes: affinity interaction of L and T, described by equation 2.1, and separation of L, T, and C based on differences in their electrophoretic velocities, v_L, v_T, and v_C. These two processes are described by the following general system of partial differential equations:

$$\begin{aligned}
&\frac{\partial L(t,x)}{\partial t} + v_L \frac{\partial L(t,x)}{\partial x} = -k_{on} L(t,x)T(t,x) + k_{off} C(t,x) \\
&\frac{\partial T(t,x)}{\partial t} + v_T \frac{\partial T(t,x)}{\partial x} = -k_{on} L(t,x)T(t,x) + k_{off} C(t,x) \\
&\frac{\partial C(t,x)}{\partial t} + v_C \frac{\partial C(t,x)}{\partial x} = -k_{off} C(t,x) + k_{on} L(t,x)T(t,x)
\end{aligned} \qquad 2.2$$

where L, T, and C are concentrations of L, T, and C, respectively; t is time passed since the beginning of separation; x is the distance from the injection end of the capillary; ∂t and ∂x are partial derivations by time t and spatial coordinate x, respectively. System 2.2 describes the two basic processes, which are always present in KCE. Depending on species studied and a specific analytical setup, other processes, such as binding with complex stoichiometry, diffusion, adsorption to capillary walls can play significant roles in KCE. In such cases, mathematical terms, describing additional processes, must be added to system 2.2. The solution of system 2.2 depends on the initial and boundary conditions: initial distribution of L, T, and C along the capillary and the way L, T, and C are introduced into the capillary and removed from the

capillary during separation. This solution can be found non-numerically for specific sets of initial and boundary conditions and specific assumptions.[62, 63] For KCE to be a generic approach, it is required that system 2.2 be solved for any set of conditions; such solutions can be found only numerically.

2.3 KCE Methods

We state that every set of unique initial and boundary conditions for system 2.2 defines a unique KCE method. **Table 2.1** compares 6 KCE methods: NECEEM, SweepCE, and the four new methods. The following unique and descriptive names were given to the new methods: continuous NECEEM (cNECEEM), short SweepCE (sSweepCE), plug-plug KCE (ppKCE), and short SweepCE of Equilibrium Mixtures (sSweepCEEM). The new methods were defined by arbitrarily selecting new qualitatively different sets of initial and boundary conditions. The table contains drawings, which schematically illustrate initial and boundary conditions for each method. It also contains representative functions $L(t)$, $T(t)$, and $C(t)$ for a fixed x for each method. The notion of "equilibrium mixture" refers to the mixture of L, T, and C at equilibrium, typically prepared outside the capillary. The concentrations of the three components, $\tilde{T}$, $\tilde{L}$, and $\tilde{C}$, in the equilibrium mixture are interconnected through the equilibrium dissociation constant, K_d, as $K_d = (\tilde{T}\tilde{L}) / \tilde{C}$. As an example, we assume than $v_T > v_L$.

KCE method	Schematic representation of initial and boundary conditions	Simulated concentration profiles

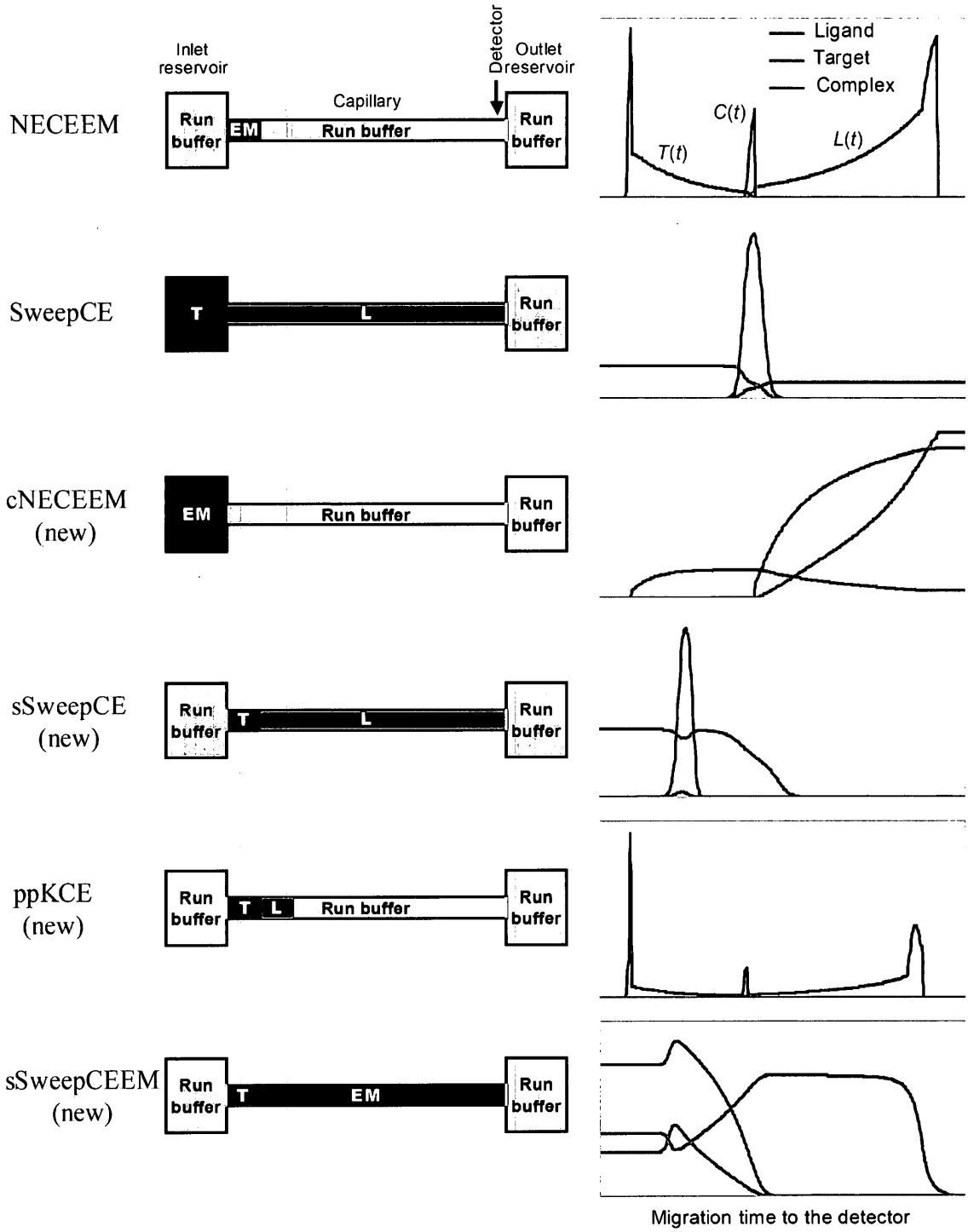

Table 2.1 Summary of KCE methods. T = Target, L = Ligand, C = Complex, EM = Equilibrium Mixture

In NECEEM, a short plug of the equilibrium mixture is injected into the inlet of the capillary, which is pre-filled with the run buffer. Separation is carried out with both inlet and outlet reservoirs containing the run buffer only. C continuously dissociates during electrophoresis. If separation is efficient, re-association of T and L can be neglected. The resulting concentration profiles (time dependencies of concentrations for a fixed x) contain three peaks of T, C, and L and two exponential "smears" of L and T, which occur from the dissociation of C.

In SweepCE, the capillary is filled with L, while the inlet reservoir contains T and the outlet reservoir contains a run buffer. During electrophoresis, T continuously moves through L, causing continuous binding of T to L. Although binding is a prevalent process in SweepCE, dissociation of C can also contribute to the resulting concentration profiles, which contain a single peak of C and plateaus of T and L.

In cNECEEM, the inlet reservoir is filled with the equilibrium mixture while the capillary and the outlet reservoir contain the run buffer. During electrophoresis, C is separated from T, which moves faster, and from L, which moves slower. As a result, C continuously dissociates inside the capillary. Although dissociation is a prevalent process in cNECEEM, re-association can also contribute to the resulting concentration profiles, which are represented by smooth functions of $T(t)$, $L(t)$, and $C(t)$ with no pronounced peaks.

In sSweepCE, a short plug of T is injected into the capillary pre-filled with L. Both inlet and outlet reservoirs contain the run buffer. T moves through L during electrophoresis causing

both association of T and L and dissociation of resulting C to occur. The concentration profiles of T and C are peak-like, while that of L is a smooth function.

In ppKCE, the plugs of L and T are injected into the capillary pre-filled with the run buffer. The inlet and outlet reservoirs contain the run buffer as well. During electrophoresis T moves through L causing the formation of C. When the zone of T passes L, C starts to dissociate. ppKCE can be considered as a functional hybrid of NECEEM and sSweepCE. The resulting concentration profiles resemble those of NECEEM with a smaller peak of C and "smears" of T and L.

In sSweepCEEM, a short plug of T is injected into the capillary pre-filled with the equilibrium mixture. Both inlet and outlet reservoirs contain the run buffer. During electrophoresis, an intricate interplay of dissociation of C and association of T and L occur resulting in sophisticated concentration profiles, which contain peaks and plateaus.

The extents of complex formation and dissociation differ in different KCE methods. KCE methods, therefore, have different accuracies of determination of k_{on} and k_{off}. For example, in NECEEM, complex dissociation prevails over complex formation, thus, making it more "sensitive" to k_{off} than k_{on}. In SweepCE, in contrast, complex formation can prevail over complex dissociation, making it more sensitive to k_{on} than k_{off}. The plug-plug KCE method can be tuned to have comparable accuracy of both k_{on} and k_{off} determination. The most accurate determination of all constants can be achieved if multiple KCE methods are combined in a single kinetic tool (see the next section).

Using the general concept of KCE, other KCE methods can be defined by simply selecting new sets of initial and boundary conditions. Importantly, this approach requires no serendipity but, rather, a rational (or irrational) design of conditions, which can be performed in an intuitive way schematically depicted in **Table 2.1**.

2.4 Multi-Method KCE Toolbox

Here we introduce the simultaneous use of multiple KCE methods as an integrated tool for kinetic studies of biomolecular interactions. The approach can be used for testing hypotheses about the mechanisms of interaction and finding kinetic parameters of the interaction. Conceptually, experimental electropherograms are obtained by multiple KCE methods first. A hypothetical model of interactions between L and T is suggested and the system of differential equations (system 2.2) is built. The experimental KCE electropherograms are fitted with simulated electropherograms simultaneously to obtain the best fits with one of the criteria used for non-linear regression analysis (e.g. minimum chi-square). If the quality of fitting is not satisfactory, a new hypothesis is suggested for the interaction. The procedure is repeated until a satisfying hypothesis is found. The best fits for the accepted hypothesis lead to the determination of stoichiometric and kinetic parameters of the interaction. **Figure 2.1** summarizes the general approach to the development and analytical utilization of a multi-method KCE toolbox.

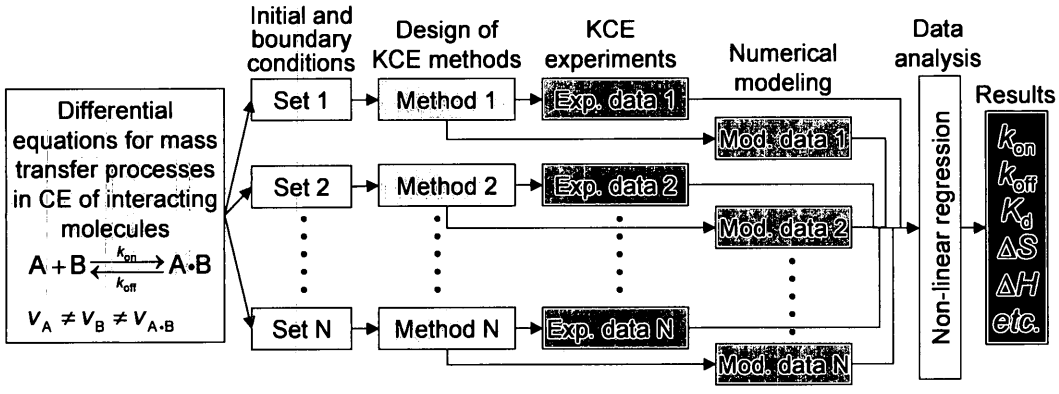

Figure 2.1 Flow chart depicting the general approach to the development and utilization of a multi-method KCE toolbox

We tested this approach using six KCE methods depicted in **Table 2.1** and a well-studied experimental system: interaction between SSB protein and ssDNA.[46, 47, 62, 64] Since the velocity of SSB in electrophoresis is greater than that of ssDNA, we assign L to ssDNA and T to SSB. Only L was fluorescently labeled in our study, so that T was not detectable while both L and C were detectable but optically indistinguishable. Simulated electropherograms, therefore, were calculated as dependencies of $L(t) + C(t)$ for x equal to the distance from the injection end of the capillary to the detector. Such simulated electropherograms could be directly compared with experimental ones.

We first tested a hypothesis that SSB and DNA interaction is described by equation 2.1. The best fit of six experimental KCE electropherograms for this hypothesis was obtained for $k_{on} = 6 \times 10^6\ M^{-1}s^{-1}$ and $k_{off} = 9 \times 10^{-4}\ s^{-1}$ (**Figure 2.2A**). Deviations between experimental and simulated electropherograms were unacceptably high for cNECEEM, sSweepCE, and sSweepCEEM, as the model was not able to reproduce the shape of fronts and peak heights, thus suggesting that the hypothesis was not valid.

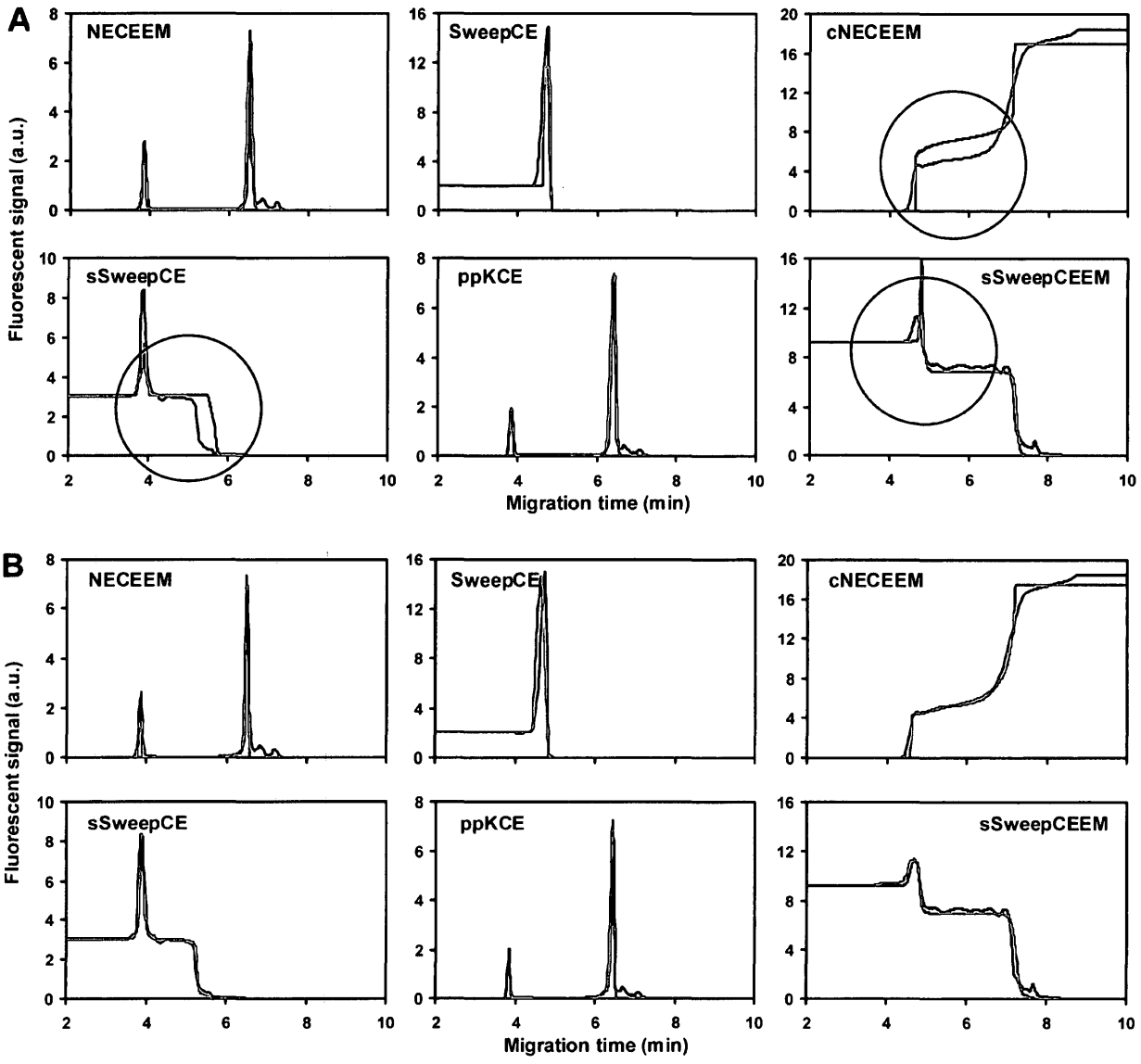

Figure 2.2 Application of the KCE toolbox to: (i) testing hypotheses about the nature of biomolecular interactions and (ii) finding rate constants of interactions. Black traces show experimental electropherograms for six KCE methods, while red traces show simulated electropherograms corresponding to the best fitting using the minimum chi-square criterion. Experimental electropherograms are identical in both panels; simulated electropherograms differ in panels A and B. Panel A presents simulated electropherograms for the unsatisfactory model, which assumes one type of interaction only. Circles indicate areas of fitting with unacceptably great deviations between experimental and simulated electropherograms. Panel B shows simulated electropherograms for the satisfying model, which assumes two types of interactions (equation 2.3). Rate constants obtained by fitting with the satisfying model are shown in expression 2.5

Second, we modified the hypothesis based on existing empirical data about protein-DNA interactions. Two types of interactions are possible between a protein and DNA: high-affinity

specific binding and low-affinity non-specific binding.[65, 66] Non-specific binding was hypothesized to occur due to electrostatic attraction between SSB and DNA, which does not necessarily involve the DNA-binding site of SSB. To account for two types of binding we modified reaction 2.1 to include two types of complexes and two sets of rate constants:

$$\begin{aligned} L + T &\underset{{}^{S}k_{off}}{\overset{{}^{S}k_{on}}{\rightleftarrows}} {}^{S}C \\ L + T &\underset{{}^{N}k_{off}}{\overset{{}^{N}k_{on}}{\rightleftarrows}} {}^{N}C \end{aligned} \qquad 2.3$$

where "S" and "N" denote specific and non-specific interactions, respectively. The system of differential equations similar to system 2.2 was built for model 2.3:

$$\begin{aligned} &\frac{\partial L(t,x)}{\partial t} + v_L \frac{\partial L(t,x)}{\partial x} = -({}^{S}k_{on} + {}^{N}k_{on})L(t,x)T(t,x) + {}^{S}k_{off}\,{}^{S}C + {}^{N}k_{off}\,{}^{N}C \\ &\frac{\partial T(t,x)}{\partial t} + v_T \frac{\partial T(t,x)}{\partial x} = -({}^{S}k_{on} + {}^{N}k_{on})L(t,x)T(t,x) + {}^{S}k_{off}\,{}^{S}C + {}^{N}k_{off}\,{}^{N}C \\ &\frac{\partial {}^{S}C(t,x)}{\partial t} + v_C \frac{\partial {}^{S}C(t,x)}{\partial x} = -{}^{S}k_{off}\,{}^{S}C + {}^{S}k_{on}L(t,x)T(t,x) \\ &\frac{\partial {}^{N}C(t,x)}{\partial t} + v_C \frac{\partial {}^{N}C(t,x)}{\partial x} = -{}^{N}k_{off}\,{}^{N}C + {}^{N}k_{on}L(t,x)T(t,x) \end{aligned} \qquad 2.4$$

Experimental KCE electropherograms were then fitted with simulated ones for the new model. The best fit was found to be in acceptable quantitative agreement with the experimental data (**Figure 2.2B**), which allowed us to accept model. The values of rate constants obtained from the non-linear regression analysis were:

$$
\begin{aligned}
{}^{S}k_{on} &= 5\times10^{5}\ M^{-1}s^{-1} \\
{}^{S}k_{off} &= 6\times10^{-4}\ s^{-1} \\
{}^{N}k_{on} &= 8\times10^{6}\ M^{-1}s^{-1} \\
{}^{N}k_{off} &= 8\times10^{-2}\ s^{-1}
\end{aligned}
\qquad 2.5
$$

The determined sets of rate constants well fit the definition of specific and non-specific interactions. Specific binding requires a specific orientation of molecules during binding, while non-specific binding occurs independently of the orientation.[67] Accordingly, ${}^{S}k_{on}$ is an order of magnitude lower than ${}^{N}k_{on}$. When specific binding occurs, it is more stable than non-specific. Accordingly ${}^{S}k_{off}$ is two orders of magnitude below ${}^{N}k_{off}$. As a result, the equilibrium dissociation constant for specific interactions, ${}^{S}K_{d} = 1.2 \times 10^{-9}$ M, is an order of magnitude lower than that of non-specific interactions, ${}^{N}K_{d} = 10^{-8}$ M.

The multi-method KCE toolbox allowed us, for the first time, to determine kinetic parameters of specific and non-specific protein-DNA interactions. To the best of our knowledge, such a toolbox represents the most powerful approach to kinetic studies of biomolecular interactions.

2.5 Discussion and Conclusions

The majority of previous attempts to utilize chromatography and electrophoresis for studying biomolecular interactions were limited to assuming equilibrium between interacting molecules.[68, 69] Not only does such an assumption limit applications to measuring equilibrium constants, but also this assumption is conceptually mistaken since separation disturbs equilibrium. We state that kinetics must be appreciated when separation methods are used for

studies of non-covalent interactions. This appreciation can dramatically enrich analytical capabilities of the methods.

To prove the benefits of the appreciation of kinetics, we introduce the concept of KCE. Capillary electrophoresis was chosen as a methodological platform as it allows separation in solution (without a solid-phase), thus, making kinetic analysis simple and accurate. KCE is defined as CE separation of molecules, which interact during electrophoresis; KCE is not a method but a general concept. To design practical KCE methods, we need to define initial and boundary conditions for interactions. The first KCE methods, NECEEM and SweepCE, were "discovered" by chance. The general concept of KCE provides a "recipe" for rational design of KCE methods. In this work, we used this recipe to define four new KCE methods.

Using a numerical modeling approach allowed us to build a multi-method KCE toolbox for kinetic studies. Different KCE methods have different accuracies for different kinetic parameters. When used together as an integrated tool, KCE methods provide a powerful way of testing hypotheses and accurately calculating binding parameters.

To conclude, we foresee that KCE methods will find multiple applications in fundamental studies of biomolecular interactions, designing clinical diagnostics, and the development of affinity probes and drug candidates. New applications will emerge with further development of KCE.

2.6 Materials and Methods

2.6.1 Chemicals and Materials

Single-stranded DNA binding protein (SSB) from *E. coli* and buffer components were from Sigma-Aldrich (Oakville, ON). A fluorescently-labeled 40-mer DNA (FAM-5'-CTTCTGCCCGCCTCCTTCCTTCCAACCTTCATCAGCCACC-3') was custom-synthesized by IDT (Coralville, IA, USA). Fused-silica capillaries were purchased from Polymicro (Phoenix, AZ). All aqueous solutions were made using the Milli-Q quality deionized water and filtered through a 0.22 μm filter (Millipore, Nepean, ON).

2.6.2 Instrumentation

All CE procedures were performed using the following instrumentation and common settings and operations unless otherwise stated. CE was carried out with a P/ACE MDQ apparatus (Beckman Coulter, Mississauga, ON) equipped with a fluorescence detector; a 488-nm line of an Ar-ion laser was utilized to excite fluorescence. A 50-cm long (40 cm to the detection window) uncoated fused silica capillary with an inner diameter of 75 μm and outer diameter of 360 μm was used. The run buffer for electrophoresis was 50 mM Tris-HCl at pH 8.2. The capillary was rinsed with the run buffer for 2 min prior to each run. Electrophoresis was carried out for a total of 10 min by an electric field of 400 V/cm with a positive electrode at the injection end of the capillary; the direction of the electroosmotic flow was from the inlet to the outlet reservoir. The temperature of the capillary and samples was maintained at 20 ± 0.1 °C. At the end of each run, the capillary was rinsed with 0.1 M NaOH for 2 min, followed by a rinse with deionized water for 2 min.

2.6.3 Solutions of SSB and DNA

Solutions of 100 nM SSB and 200 nM DNA as well as equilibrium mixtures (total of 100 nM SSB and 200 nM DNA) were prepared in the CE run buffer (50 mM Tris-HCl, pH 8.2).

2.6.4 NECEEM

The inlet and outlet reservoirs contained the run buffer, and the capillary was pre-filled with the run buffer. A plug of the SSB-DNA equilibrium mixture was injected into the capillary by a pressure pulse of 5 s × 0.5 psi; the length and volume of the injected equilibrium mixture were 7 mm and 30 nL, respectively.

2.6.5 SweepCE

The capillary was pre-filled with the solution of DNA. The inlet reservoir contained the solution of SSB. The outlet reservoir contained the run buffer.

2.6.6 Continuous NECEEM (cNECEEM)

The outlet reservoir contained the run buffer, and the capillary was pre-filled with the run buffer. The inlet reservoir contained the SSB-DNA equilibrium mixture.

2.6.7 Short SweepCE (sSweepCE)

The capillary was pre-filled with a solution of DNA. The inlet and outlet reservoirs contained the run buffer. A plug of the SSB solution was injected into the capillary by a pressure pulse of 5 s × 0.5 psi; the length and volume of injected plug were 7 mm and 30 nL, respectively.

2.6.8 Plug-plug KCE (ppKCE)

The inlet and outlet reservoirs contained the run buffer, and the capillary was pre-filled with the run buffer. First, a plug of the DNA solution was injected into the capillary by a pressure pulse of 10 s × 0.5 psi. The length and volume of the plug were 14 mm and 60 nL,

respectively. Second, a plug of the SSB solution was injected into the capillary by a pressure pulse of 5 s × 0.5 psi. The length and volume of the plug were 7 mm and 30 nL, respectively.

2.6.9 Short SweepCE of Equilibrium Mixture (sSweepCEEM)

The inlet and outlet reservoirs contained the run buffer, and the capillary was pre-filled with the equilibrium mixture. A plug of the SSB solution was injected into the capillary by a pressure pulse of 5 s × 0.5 psi; the length and volume of injected plug were 7 mm and 30 nL, respectively.

2.6.10 Numerical Modeling

A computer program for numerical simulation of KCE electropherograms was written in Pascal. Rate constants were determined by non-linear regression analysis using the minimum chi-square method.

Chapter 3. Plug-Plug Kinetic Capillary Electrophoresis

The presented material was published previously. Adapted with permission from Okhonin, V.; **Petrov, A. P.**; Berezovski, M.; Krylov, S. N., Plug-plug kinetic capillary electrophoresis: method for direct determination of rate constants of complex formation and dissociation. *Anal Chem* **2006,** *78* (14), 4803-10.

Contribution to the article: performed all ppKCE experiments, participated in data analysis, prepared figures, participated in manuscript writing

3.1 Introduction

Non-covalent molecular interactions play a key role in all regulatory biological processes, for example: cell recognition, immune response, signal transduction, gene expression, DNA replication, and others.[70-72] Finding molecules capable of non-covalently binding therapeutic targets is the principle approach in modern drug development.[73] Furthermore, many analytical techniques and devices used in research and disease diagnostics (e.g. immunoassays, biosensors, and DNA hybridization analysis) are based on the formation of non-covalent molecular complexes.[74] Hence, efficient methods for studying non-covalent interactions are pivotal to our progress in many areas of modern physical and life sciences.

The formation and dissociation of a non-covalent complex C between molecules A and B are characterized by a bimolecular rate constant k_{on}, and a unimolecular rate constant, k_{off}, of the forward and reverse reactions, respectively:

$$A + B \underset{k_{off}}{\overset{k_{on}}{\rightleftharpoons}} C \qquad 3.1$$

Knowledge of k_{on} and k_{off} is essential for: (i) understanding the dynamics of biological processes, (ii) determining the pharmacokinetics of target-binding drugs, and (iii) designing quantitative affinity analyses.

Lately, we have focused on capillary electrophoresis-based kinetic methods for studies of non-covalent molecular interactions. These efforts are based on the insight that if A is allowed to interact with B during electrophoresis, the resulting electropherograms will have a memory of this interaction. Thus, we concentrated on defining different ways of interaction and developing approaches to retrieving kinetic parameters from electropherograms. We term this area of research Kinetic Capillary Electrophoresis (KCE) and define KCE as CE separation of species, which interact during electrophoresis.

The aim of the present work was to design a KCE method capable of directly measuring both k_{on} and k_{off} without the need for non-linear regression analysis. The new method is termed plug-plug Kinetic Capillary Electrophoresis (ppKCE). Conceptually, short plugs of solutions of A and B are injected into the capillary sequentially; the component with lower mobility is injected first. When the voltage is applied, the faster moving component passes through the slower moving component resulting in complex formation. Eventually, the electrophoretic zones of A and B are separated and the complex starts dissociating. The resulting electropherogram is qualitatively similar to that of NECEEM: it has peaks of A, B, and C and "smears" of A and B dissociated from C. However, since ppKCE does not start with the equilibrium mixture of A and B, the resulting electropherogram does not have a "memory" of K_d but rather has a memory of k_{on} and k_{off}. Both k_{on} and k_{off} can, thus, be calculated from a single ppKCE electropherogram using areas of peaks and smears and migration times of peaks. The mathematical analysis uses three simplifying assumptions for reaction 3.1. First, we assume a simple 1:1 stoichiometry of interaction between A and B; for higher-order stoichiometries, numerical modeling of KCE data has to be used.[75] Second, we assume that only the forward reaction occurs when the zone of B

moves through that of A. Finally, we assume that only the reverse process in reaction 3.1 occurs after the zones of A and B are separated. In this work, the ppKCE method was used to calculate k_{on} and k_{off} for interaction between a single-stranded DNA-binding protein and DNA. The new method is simple, fast, and informative. It does not require expertise in mathematical modeling and, thus, can be used by a broad community of researchers.

3.2 Plug-Plug KCE

We define ppKCE as the method in which A and B are introduced into a capillary as a sequence of two short plugs when the capillary is pre-filled with the run buffer and both inlet and outlet reservoirs also contain the run buffer (**Figure 3.1**). A slower moving component is injected first. In this work we assume that A is slower than B. A spacer plug of a bare buffer can be introduced between the plugs A and B to prevent mixing of A and B and the start of reaction 3.1 before the beginning of electrophoresis.

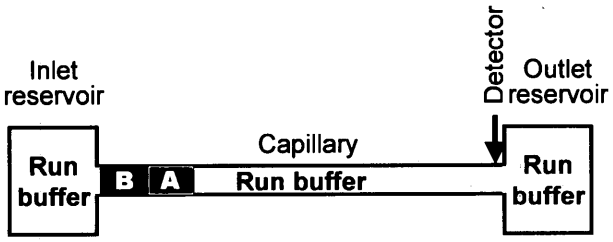

Figure 3.1 Schematic representation of initial and boundary conditions in ppKCE

3.3 Numerical Simulation of ppKCE

To demonstrate qualitative features of ppKCE, we simulated $A(t,x)$, $B(t,x)$, and $C(t,x)$ numerically for a fixed x as described elsewhere.[76] These dependencies were used to build simulated ppKCE electropherograms, which represent a superposition of $A(t)$, $B(t)$, and $C(t)$ for x which is equal to the distance from the capillary inlet ($x = 0$) to the detector.

Figure 3.2 shows simulated electropherograms (dependencies of $A(t)$, $B(t)$, and $C(t)$) for different k_{off} and k_{on}. Please, note the difference in scales of the y-axes in **Figure 3.2**. **Figure 3.2a** demonstrates the influence of k_{off} on electropherograms for a constant k_{on}. Since k_{on} is constant, the amount of C formed by the time when the zones of A and B are separated does not change with changing k_{off}. The variation in k_{off} changes only the rate with which C dissociates after the zones of A and B are separated. Accordingly, increasing k_{off} leads to decreasing heights of the peak of $C(t)$ and increasing areas of the smears of $A(t)$ and $B(t)$. **Figure 3.2b** illustrates the influence of k_{on} on ppKCE electropherograms for a constant k_{off}. Increasing k_{on} results in an increasing amount of C formed, leading to decreasing peaks of $A(t)$ and $B(t)$ and a growing peak of $C(t)$.

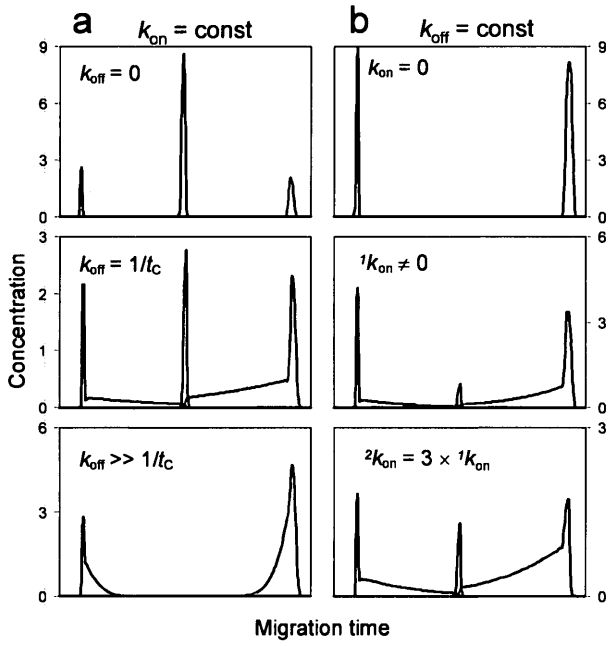

Figure 3.2 Simulated ppKCE electropherograms for: constant k_{on} and three different k_{off} (panel a) and for constant k_{off} and three different k_{on} (panel b). Red, green and blue colors correspond to $A(t)$, $C(t)$ and $B(t)$ respectively

Electropherograms in ppKCE are qualitatively similar to those in NECEEM. The difference between NECEEM and ppKCE is in the amount of C. NECEEM uses the equilibrium mixture of A and B, which has the highest possible amount of C for given concentrations of A and B. To measure k_{on}, ppKCE has to be performed so that quasi-equilibrium is not reached during the passage of the zone of B through the zone of A. As a result, the amount of C in ppKCE is lower than that in NECEEM. As was previously demonstrated for NECEEM,[63] $A(t)$ and $B(t)$ consist of two parts (**Figure 3.3a**):

$$A(t) = A_{free}(t) + A_{dis}(t)$$
$$B(t) = B_{free}(t) + B_{dis}(t) \qquad 3.2$$

$A_{free}(t)$ and $B_{free}(t)$ correspond, respectively, to A and B which do not form the complex during the mixing of the zones of A and B. $A_{dis}(t)$ and $B_{dis}(t)$ correspond, respectively, to A and B, which

result from the dissociation of C after the zones are separated. Areas of peaks and smears in the electropherogram, $\mathbf{A}_{free}$, $\mathbf{A}_{dis}$, $\mathbf{B}_{free}$, $\mathbf{B}_{dis}$, and **C**, are proportional to the amounts of corresponding species (**Figure 3.3b**).

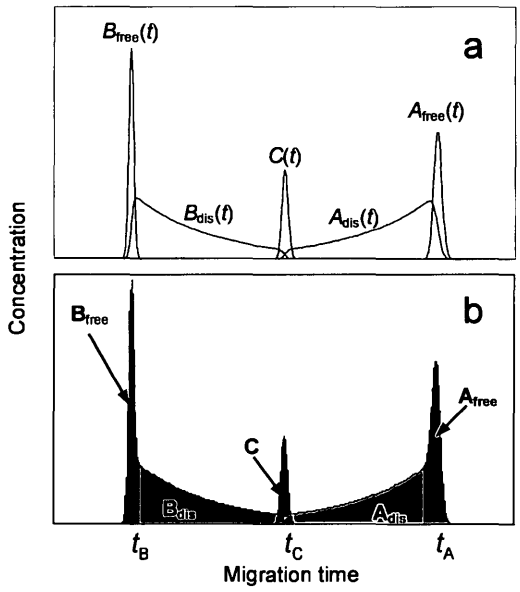

Figure 3.3 Panel a shows simulated ppKCE concentration profiles with functions $A(t)$ and $B(t)$ being presented as a superposition of free and dissociated components (see equation 3.2). Panel b illustrates measurable parameters (areas of peaks and smears and migration times of A, B, and C), which are used for the determination of k_{on} and k_{off} without non-linear regression analysis

The goal of this work was to develop a means of calculating k_{on} and k_{off} using only parameters easily measurable from a ppKCE electropherogram. These parameters are $\mathbf{A}_{free}$, $\mathbf{A}_{dis}$, $\mathbf{B}_{free}$, $\mathbf{B}_{dis}$, **C** and migration times of A, B, and C: t_A, t_B and t_C, respectively.

3.4 Determination of Rate Constants in ppKCE

3.4.1 Determination of k_{off}

The complex dissociation process is identical in NECEEM and ppKCE; therefore, approaches developed for the calculation of k_{off} in NECEEM are applicable to ppKCE as well.[46, 62, 63] The most practical approach uses the areas and migration times (**Figure 3.3b**):

$$k_{off} = \ln\left(\frac{\mathbf{C}+\mathbf{A}_{dis}}{\mathbf{C}}\right)/t_C = \ln\left(\frac{\mathbf{C}+\mathbf{B}_{dis}}{\mathbf{C}}\right)/t_C \qquad 3.3$$

This non-numerical approach to the determination of k_{off} requires the assumption that no re-binding of A and B occurs when the electrophoretic zones of A and B are separated.

3.4.2 Determination of k_{on}

Determination of k_{on} in ppKCE without non-linear regression analysis requires the development of a new mathematical approach. The details on development and validation of such approach can be found elsewhere.[75] When the zone of B passes through the zone of A, the forward reaction (the formation of C) occurs. For the approach to work, we make a simplifying assumption that the reverse reaction (the dissociation of C) is negligible during this time.

When the abovementioned assumption is satisfied the k_{on} can be calculated from the following expression[75]:

$$k_{on} = \varepsilon(v_B - v_A)/([A]l_A) \qquad 3.4$$

The value of ε can be determined from equation 3.5,[75] using the Microsoft Excel program as described in section 3.8.

$$\mathbf{A}_{free}/(\mathbf{A}_{free}+\mathbf{A}_{dis}+\mathbf{C}) = 1/\varepsilon \times \ln\left\{(\exp(\varepsilon)-1)\exp\left(-\varepsilon \times ([B]l_B/([A]l_A))\right)+1\right\} \qquad 3.5$$

In this equation, all parameters but ε are either controlled or measurable. The velocities in equation 3.4 can be replaced by the effective capillary length L, divided by corresponding migration times (t_B or t_A):

$$k_{on} = \varepsilon L(1/t_B - 1/t_A)/([A]l_A) \quad 3.6$$

This allows determination of k_{on} when $\mathbf{A}_{free}$, $\mathbf{A}_{dis}$, $\mathbf{C}$, t_B, and t_A are determined from a ppKCE electropherogram. The other four parameters, [B], [A], l_B, and l_A, are controlled by an experimentalist.

3.4.3 Satisfying the Model Assumptions

Table 3.1 can be used to identify a range of experimental conditions that satisfy the assumptions of the model.[75] **Table 3.1** lists upper suitable limits for k_{off} as a function of k_{on}, time of zones of A and B passing through each other (t_{pass}), and the highest of the concentrations of A and B (Max (A, B)). To test whether the experimental conditions are acceptable for the model, the user has to choose the column with the concentration closest to the highest of the two concentrations ([A] and [B]) used in experiment, then choose the row with the k_{on} value closest to the anticipated k_{on} value and finally choose the subrow with t_{pass} which correspond to the given experimental conditions. The corresponding value in the column would give the upper acceptable limit of the k_{off} value for the mathematical model to work. If the dissociation is faster than the found upper limit of acceptable k_{off}, one should choose more appropriate conditions to satisfy the assumptions. First, a separation buffer can be found, which facilitates a greater differential velocity of A and B and, thus, a shorter t_{pass}. Second, the initial concentrations of A and B can be decreased. Finally, the lengths of the plugs of A and B can be decreased. We anticipate that suitable conditions will be found for most types of biomolecular interactions.

The conditions found from **Table 3.1** to satisfy the assumptions for the model also guarantee that the equilibrium is not reached. In addition, the fact that the equilibrium is not reached can be confirmed by comparing NECEEM and ppKCE data. If the C/A_{free} ratio is

smaller for ppKCE than that for NECEEM then the equilibrium is not reached (the maximum ratio is achieved at equilibrium).

Table 3.1 Upper limits for k_{off} values as function of concentrations, time of electrophoretic zones passing through each other (t_{pass}), and k_{on} values

k_{on} ($M^{-1}s^{-1}$)	t_{pass} (s)	Max (A, B) (M)					
		10^{-4}	10^{-5}	10^{-6}	10^{-7}	10^{-8}	10^{-9} - 10^{-12}
10^3	1	1.00×10^{0}	1.00×10^{0}	1.00×10^{0}	1.00×10^{0}	1.00×10^{0}	1.00×10^{0}
	10	1.00×10^{-1}	1.00×10^{-1}	1.00×10^{-1}	1.00×10^{-1}	1.00×10^{-1}	1.00×10^{-1}
	40	1.25×10^{-2}	2.50×10^{-2}	2.50×10^{-2}	2.50×10^{-2}	2.50×10^{-2}	2.50×10^{-2}
	80	3.13×10^{-3}	1.25×10^{-2}	1.25×10^{-2}	1.25×10^{-2}	1.25×10^{-2}	1.25×10^{-2}
10^4	1	1.00×10^{0}	1.00×10^{0}	1.00×10^{0}	1.00×10^{0}	1.00×10^{0}	1.00×10^{0}
	10	2.00×10^{-2}	1.00×10^{-1}	1.00×10^{-1}	1.00×10^{-1}	1.00×10^{-1}	1.00×10^{-1}
	40	1.25×10^{-3}	1.25×10^{-2}	2.50×10^{-2}	2.50×10^{-2}	2.50×10^{-2}	2.50×10^{-2}
	80	3.13×10^{-4}	3.13×10^{-3}	1.25×10^{-2}	1.25×10^{-2}	1.25×10^{-2}	1.25×10^{-2}
10^5	1	2.00×10^{-1}	1.00×10^{0}	1.00×10^{0}	1.00×10^{0}	1.00×10^{0}	1.00×10^{0}
	10	2.00×10^{-3}	2.00×10^{-2}	1.00×10^{-1}	1.00×10^{-1}	1.00×10^{-1}	1.00×10^{-1}
	40	1.30×10^{-4}	1.25×10^{-3}	1.25×10^{-2}	2.50×10^{-2}	2.50×10^{-2}	2.50×10^{-2}
	80	3.13×10^{-5}	3.13×10^{-4}	3.13×10^{-3}	1.25×10^{-2}	1.25×10^{-2}	1.25×10^{-2}
10^6	1	2.00×10^{-2}	2.00×10^{-1}	1.00×10^{0}	1.00×10^{0}	1.00×10^{0}	1.00×10^{0}
	10	2.00×10^{-4}	2.00×10^{-3}	2.00×10^{-2}	1.00×10^{-1}	1.00×10^{-1}	1.00×10^{-1}
	40	1.30×10^{-5}	1.30×10^{-4}	1.25×10^{-3}	1.25×10^{-2}	2.50×10^{-2}	2.50×10^{-2}
	80	3.13×10^{-6}	3.13×10^{-5}	3.13×10^{-4}	3.13×10^{-3}	1.25×10^{-2}	1.25×10^{-2}
10^7	1	2.00×10^{-3}	2.00×10^{-2}	2.00×10^{-1}	1.00×10^{0}	1.00×10^{0}	1.00×10^{0}
	10	2.00×10^{-5}	2.00×10^{-4}	2.00×10^{-3}	2.00×10^{-2}	1.00×10^{-1}	1.00×10^{-1}
	40	1.30×10^{-6}	1.30×10^{-5}	1.30×10^{-4}	1.25×10^{-3}	1.25×10^{-2}	2.50×10^{-2}
	80	3.13×10^{-7}	3.13×10^{-6}	3.13×10^{-5}	3.13×10^{-4}	3.13×10^{-3}	1.25×10^{-2}

3.5 Application of ppKCE to Protein-Ligand Complexes

To demonstrate the practical application of the method, we used interaction between SSB protein and ssDNA. DNA was fluorescently labeled to facilitate sensitive detection. SSB did not have a fluorophore and was not detectable; the complex of SSB with fluorescently labeled DNA was detectable. Under separation conditions that were chosen, DNA was migrating slower than SSB, so we will be referring to DNA and SSB as A and B components, respectively, to be consistent with the previous theoretical consideration. An experimental ppKCE electropherogram for the SSB-DNA interaction is shown in **Figure 3.4**. All experimental values presented below without deviations correspond to the data in this figure. To determine the left boundary of the peak of $\mathbf{A}_{free}$, the ppKCE electropherogram was compared with a control electropherogram with DNA only. The boundary between C and $\mathbf{A}_{dis}$ can be accurately determined using fluorescence anisotropy as we described earlier.[62] Relative deviations of peak areas associated with uncertainties of the boundaries are typically within 10%. The values of $\mathbf{A}_{dis}$ and $\mathbf{A}_{free}$, the apparent value of **C** ($\mathbf{C}_{app}$), and the migration time of C and A were obtained from the electropherogram: $\mathbf{A}_{dis} = 121$, $\mathbf{A}_{free} = 128$, $\mathbf{C}_{app} = 15.9$, and $t_C = 204$ s. $\mathbf{C}_{app}$ differs from **C** by a relative fluorescence quantum yield q of C with respect to that of free A: $\mathbf{C}_{app} = \mathbf{C} \times q$. The value of q was calculated by measuring the total areas in two electropherograms. The first was obtained from A in the presence of B (**Figure 3.4**) and the second was in the absence of B (not shown). The total area in the absence of B was $\mathbf{A} = 294$. The total areas in the 2 electropherograms should be identical if $\mathbf{C}_{app}$ is divided by q:

$$\mathbf{A} = \mathbf{C}_{app}/q + \mathbf{A}_{dis} + \mathbf{A}_{free} \qquad 3.7$$

From this equation we can find q:

$$q = \mathbf{C}_{app}/(\mathbf{A} - \mathbf{A}_{dis} - \mathbf{A}_{free}) \qquad 3.8$$

The relative quantum yield calculated from equation 3.8 was: $q = 0.35$. This allowed us to obtain $\mathbf{C} = \mathbf{C}_{app}/q = 45$. This value along with the above values for $\mathbf{A}_{dis}$, $\mathbf{A}_{free}$ and t_C were used in the following calculation of the rate constants. For simplicity, we assumed that only one effective k_{on} and k_{off} constants exist.

The average k_{off} value and its experimental deviation, $k_{off} = (6.4 \pm 0.8) \times 10^{-3}$ s^{-1}, were calculated using equation 3.3 from 5 consecutive experiments similar to the one depicted in **Figure 3.4**.

To determine k_{on}, we used the same values of $\mathbf{A}_{dis}$, $\mathbf{A}_{free}$, $\mathbf{C}$, as well as [A] = 2.0×10^{-7} M, [B] = 2.0×10^{-7} M, $l_A = 0.40$ cm, $l_B = 0.40$ cm, $t_A = 400$ s, $t_B = 138$ s, and $L = 40$ cm. The value

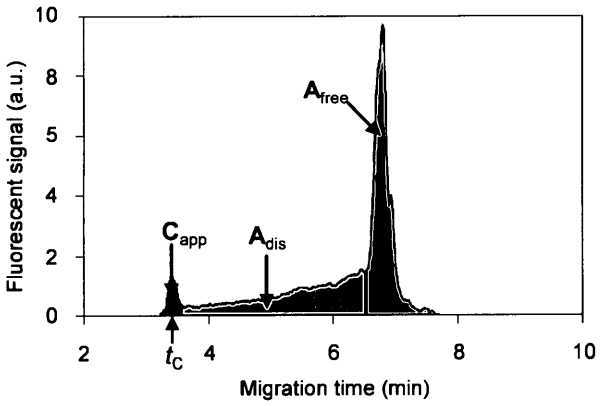

Figure 3.4 Experimental electropherogram for 200 nM SSB with 200 nM fluorescently labeled DNA interaction using ppKCE method. The areas used in analysis are color-coded: green for the complex, pink for the decay and red for the unreacted DNA

of ε was calculated from expression 3.5 using the "Goal Seek" procedure in Excel (see section 3.8). For the electropherogram depicted in **Figure 3.4**, the value of ε was equal to 1.23.

The values of k_{off} and k_{on} determined by ppKCE were found to be in good agreement with those obtained by other KCE methods.[46, 47, 62] The previously reported k_{off} is slightly higher because CE separations in the earlier works were performed at higher temperatures using CE instrumentation with no temperature control. It is instructive to compare our data on SSB-DNA binding with those published by others. LeCaptain *et al.*[77] used CE coupled with single molecule fluorescence correlation spectroscopy to measure K_d = 2 nM. This result is close to ours: $K_d = k_{off}/k_{on} = 6.4 \times 10^{-3}/2.9 \times 10^{6} = 2.2 \times 10^{-9}$ M. The data for k_{on} and k_{off} for SSB-DNA interactions are scarce, but those, which are available, show tremendous differences depending on substrates and experimental conditions used. SPR data show that in the non-cooperative mode of binding, SSB binds DNA with the following rate constants: $k_{off} = 1.34 \times 10^{-4}$ s^{-1} and $k_{on} = 1.1 \times 10^{6}$ $M^{-1}s^{-1}$. This result is comparable with ours in terms of k_{on}; the k_{off} obtained by SPR is lower, most likely due to the lower pH.[78] The stopped-flow measurements on long DNA revealed the k_{on} value of 2.1×10^{8} $M^{-1}s^{-1}$, which differs two orders of magnitude from SPR and ppKCE data. This difference is most likely due to the fact that SSB exhibits highly cooperative binding for long DNA substrates.[79] Kozlov and Lohman reported that depending on the substrate and experimental conditions k_{on} for SSB-DNA interaction can vary between 10^3 and 10^8 $M^{-1}s^{-1}$.[80] Our own data and the results by others indicate that the kinetic parameters of protein-DNA interactions are so sensitive to change in experimental conditions, such as temperature and pH, that it is imperative that the rate constants be measured *de novo* when experimental conditions change. This emphasizes the need for simple, reliable, sensitive, and fast methods for

kinetic studies of protein-DNA interactions. The methods of KCE augment the arsenal of tools available for such studies.

3.6 Conclusions

In this work, we developed a novel KCE method for direct determination of rate constants of complex formation and dissociation from one experimental electropherogram without performing non-linear regression analysis so that the method does not require expertise in mathematical modeling. The method presented is simple and robust. It requires only nanoliter volumes of reagents and can be readily adjusted for different ranges of both constants. We believe that this method will be useful for screening large libraries for drug candidates as well as the development of novel research and diagnostic tools.

3.7 The use of Microsoft Excel for Calculations of k_{on} and k_{off}

It is possible to find ε from equation 3.5, using the embedded standard procedure "Goal Seek" in the "Tools" menu of Microsoft Excel. Before calling the procedure, all experimental values required for calculations have to be entered in individual cells on an Excel spreadsheet. In addition, the initial value of ε for the first iteration has to be entered; $\varepsilon = 1$ can be used as a default number. Another cell should contain the difference between the left hand side and the right hand side of equation 3.5. To increases the accuracy of numerical calculations, this difference can be multiplied by a large number, for example 1000. The "Goal Seek" procedure can be then called. The parameters in the "Parameter" menu should be setup in the following way. The cell containing the difference between the left hand side and right hand side of equation 3.5 should be chosen for the "Set Cell" parameter. The "To Value" parameter should be set to 0. The "By changing cell" parameter should be referenced to the cell containing the initial

value of ε.The "Goal Seek" function would then give the value of ε required for the determination of k_{on} with equation 3.6. An example of such Excel spreadsheet can be found in the Research section of the following web page: www.chem.yorku.ca/profs/krylov.

For routine work, such as screening large libraries of compounds for their ability to bind a target, it is possible to construct a family of diagrams of the $A_{free}/(A_{free} + A_{dis} + C)$ dependence on ε at fixed B_{in}/A_{in} ratios from which ε can be determined. An example of such diagrams is shown in **Figure 3.5**.

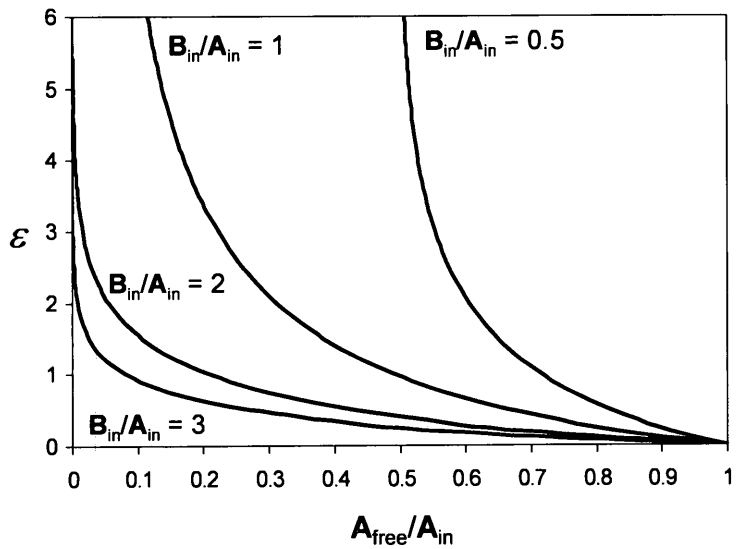

Figure 3.5 Example of diagrams which can serve for rapid determination of ε

3.8 Materials and methods

3.8.1 Chemicals and Materials

Single-stranded DNA binding protein (SSB) from *E. coli* and buffer components were from Sigma-Aldrich (Oakville, ON). A fluorescently-labeled 15-mer DNA (fluorescein-5'-GCGGAGCGTGGCAGG-3') was a gift of Dr. Y. Li (McMaster University, Canada). Fused-silica capillaries were purchased from Polymicro (Phoenix, AZ). All aqueous solutions were

made using the Milli-Q quality deionized water and filtered through a 0.22 μm filter (Millipore, Nepean, ON).

3.8.2 Instrumentation

All CE procedures were performed using the following instrumentation and common settings and operations unless otherwise stated. CE was carried out with a P/ACE MDQ apparatus (Beckman Coulter, Mississauga, ON) equipped with a fluorescence detector; a 488-nm line of an Ar-ion laser was utilized to excite fluorescence. A 50-cm long (40 cm to a detection window) uncoated fused silica capillary with an inner diameter of 75 μm and outer diameter of 360 μm was used. The sample buffers and the electrophoresis run buffer were identical: 25 mM sodium tetraborate at pH 9.3. The capillary was rinsed with the run buffer for 2 min prior to each run. Electrophoresis was carried out for a total of 10 min by an electric field of 600 V/cm with a positive electrode at the injection end of the capillary; the direction of the electroosmotic flow was from the inlet to the outlet reservoir. The temperature of the capillary was maintained at 15 ± 0.1 °C. At the end of each run, the capillary was rinsed with 0.1 M NaOH for 2 min, followed by a rinse with deionized water for 2 min.

3.8.3 Plug-Plug KCE (ppKCE)

The inlet and outlet reservoirs contained the run buffer, and the capillary was pre-filled with the run buffer. Injections were carried out by voltage so that plug lengths depended on both the velocity of the electroosmotic flow (common for all species) and electrophoretic velocities of injected specie. First, a plug of the DNA solution was injected into the capillary by a voltage pulse of 6 s × 10 kV. The length and volume of the plug were 2 mm and 8 nL, respectively. Second, to prevent the pre-mixing caused by the differential electrophoretic mobility of DNA

and SSB, we injected a short plug of the bare run buffer. The injection was carried out by a voltage pulse of 8 s × 10 kV. Third, a plug of the SSB solution was injected into the capillary by a voltage pulse of 3 s × 10 kV. The length and volume of the plug were 3 mm and 12 nL, respectively. The differences in plug lengths are caused by the differences in electrophoretic mobilities of SSB and DNA. The ends of the capillary were inserted in the inlet and outlet reservoirs, and the electric field was applied to run electrophoresis. Areas of electrophoretic peaks were divided by migration times of corresponding species to ensure that areas are proportional to the amounts of the species.

3.8.4 Determination of k_{on} and k_{off}

The k_{on} and k_{off} values were determined by inputting experimentally measured parameters into the Microsoft Excel software program, which uses the formulas, provided in sections 3.4.1 and 3.4.2

Chapter 4. Predictive measure of quality of micromixing

The presented material was published previously. Parts of the text and figures with and without modifications were taken from the following article:
Petrov, A. P.; Dodgson, B. J.; Cherney, L. T.; Krylov, S. N., Predictive measure of quality of micromixing. *Chem Commun* **2011,** *47* (27), 7767-7769.

Reproduced by permission of The Royal Society of Chemistry

Contribution to the article: performed all experiments, performed data analysis, prepared figures, participated in manuscript writing

4.1 Introduction

As mentioned before, one of the advantages of capillary electrophoresis is the nanoliter consumption of reagents. To fully take advantage of nanoliter consumption the mixing of reagents outside of a capillary should be avoided. Premixing in a test tube requires a minimum of a microliter volume thus 90-99% of the premixed sample would not be used for capillary analysis. To solve this problem, the reactants should be sequentially injected and mixed inside a capillary. In such a scenario, only nanoliter volumes of reactants would be consumed. This is important for expensive reagents, such as proteins or combinatorial libraries, which cannot be obtained in high amounts.

Recently, our group has introduced a generic method for mixing of reagents inside a capillary termed Transverse Diffusion of Laminar Flow Profiles (TDLFP).[81] The concept of mixing of reagents by TDLFP is shown in **Figure 4.1**. To mix reactants, they are sequentially injected into a capillary by pressures high enough to make the injection flow parabolic. The injection time is short enough, so that the flow front stays parabolic and does not diffuse out to the walls. In such a case, every injected plug would penetrate the previously injected plug. The transverse diffusion would then mix the reactants by eliminating the concentration profiles in this direction.

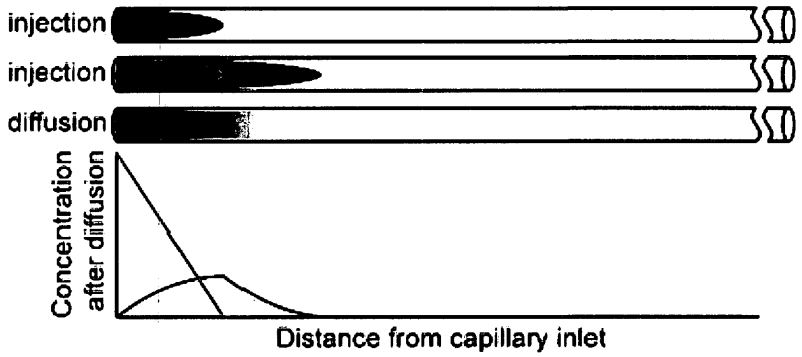

Figure 4.1 Schematic representation of in-capillary mixing of two solutions, blue and red, by TDLFP. The top panel shows the two steps in mixing: sequential injection of the solutions and their transverse diffusion. The bottom panel shows the concentration distribution after this mixing

For KCE methods, the TDLFP effect can be both advantageous and disadvantageous. While the described effect allows mixing of reagents inside the capillary and allows automation of mixing and low sample consumption it is not always a desirable one. In some KCE methods, such as the previously described ppKCE, no premixing of reactants should occur prior to separation. In this method, the TDLFP effect is undesirable and should be either avoided or accounted for in subsequent analysis of the data.

This, however, presents a problem since there was no parameter that could quantitatively describe the quality of mixing in a capillary and predict the product yield. This problem is not limited to the in-capillary mixing, but concerns mixing in microreactors in general.

4.2 Micromixing vs Macromixing

Reaction parameters, such as reaction rate and product yield, depend on the quality of reactants' mixing; therefore, the understanding and optimization of reactions require *predictive* quantitative measures of the quality of mixing, which can predict the reaction parameters. In macroreactors, mixing by mechanical agitation (macromixing) is used to randomly break

solutions into microvolumes and, thus, aid the final mixing of reactants by diffusion (micromixing). The random nature of macromixing usually makes the entire process of mixing in macroreactors stochastic. Therefore, stochastic approaches are applicable to characterizing the quality of mixing in macroreactors. A number of such approaches have been developed and extensively reviewed.[82, 83] A classical example is the Danckwerts approach, which introduces the intensity of segregation, a predictive stochastic measure of mixing, linearly related to the reaction rate.[84] Microreactors are an attractive media for chemical synthesis[85-95] and analysis[96, 97], which have become practical due to technological advances in their manufacturing. Technical difficulties of mechanical agitation in small volumes make macromixing in microreactors combersome.[98] On the other hand, micromixing in such reactors may be sufficiently fast, which, in turn, makes macromixing unnecessary.[99, 100] Micromixing is not a random process in the scale of the microreactor – the deterministic nature of diffusion leads to well-defined non-random distributions of the reactants throughout the microreactor's volume.[98, 101] As a result, the predictive stochastic measures of mixing developed for macromixing are not applicable to micromixing. The quality of micromixing in microreactors was addressed in significantly fewer works. A standard statistical function, coefficient of variation, and some empirical functions, were used as quantitative measures of micromixing.[102, 103] However, these measures have never been shown to predict any reaction parameter, e.g. the rate or product yield of the reaction.

4.3 Parameter for Characterizing Efficiency of Micromixing

Here we introduce the first predictive quantitative measure of micromixing, Quantitative Overlap (*QO*) and demonstrate its predictive ability. In this proof-of-principle work, *QO* was experimentally examined for a bimolecular reaction conducted in a capillary microreactor with discontinuous mixing. This theoretically calculated measure turned out to be proportional to the

experimentally determined relative product yield. Due to the generic nature of *QO*, it can be used to characterize micromixing for different reactions in various microreactors, with some restrictions specified below. One of the potential practical applications of *QO* is obvious: the theoretical optimization of microreactors for maximized product yield. Other applications are still to be indentified. We also foresee that new quantitative characteristics of micromixing could be introduced to predict reaction parameters other than product yield.

For a quantitative measure to be suitable for comparing efficiencies of micromixing in different systems (reactions and reactors), it should change within the same interval (for example, between 0 and 1) regardless of the system specifics. To correlate with product yield, the parameter has to be maximum for similar distributions of the reactant through the reactor and minimum when there is no non-zero volume in which all reactants are present. The definition of the measure's behavior between these two extremes can vary; therefore, different measures can be introduced to be predictive of the product yield in different systems. We present one such parameter, named quantitative overlap (*QO*), that is defined for a general case of N reactants, $R_1,\ldots, R_N$, in the following way:

$$QO(t) = \frac{1}{V}\int_V \min\left(\frac{R_1(\vec{r},t)}{\frac{1}{V}\int_V R_1(\vec{r},t)d\vec{r}},\ldots,\frac{R_N(\vec{r},t)}{\frac{1}{V}\int_V R_N(\vec{r},t)d\vec{r}}\right)d\vec{r} \qquad 4.1$$

Here $R_1,\ldots, R_N$ are concentrations of the corresponding reactants, V is the volume of the reactor, $\vec{r}$ is a vector of the spatial coordinate, and t is time. $1/V\int$ designates an operation of finding the spatial average of a function over volume V of the reactor. The "min" function in 4.1 denotes a

minimum calculated from a set of the arguments separated by the commas. Equation 4.1 depends on the number of the reactants rather than on the order of the reaction. QO is solely defined by a spatial distribution of reactants throughout the reactor and can change with time whenever the distribution changes with time. It can be strictly proved that QO defined by equation 4.1 satisfies the following: (i) $0 \leq QO \leq 1$, (ii) $QO = 0$ if and only if there is no a non-zero volume in the reactor where all reactants are present, (iii) $QO = 1$ is and only if all concentration profiles are similar to each other, and (iv) QO does not change if an empty volume is added to the system. Detailed proofs of these properties of QO are given elsewhere.[104] For example, if all concentrations are similar to each other then values of all arguments of the "min" function in 4.1 are the same in each point. This allows the "min" function to be replaced with a value of the first argument. Then, integration in 4.1 leads to $QO = 1$. **Figure 4.2** illustrates the change in QO for the changing distribution of 2 reactants in a quasi-1-dimensional reactor, including the two extreme cases of $QO = 1$ and $QO = 0$.

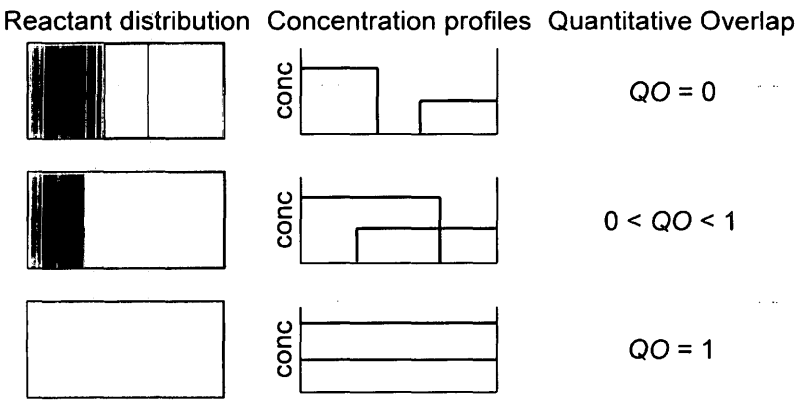

Figure 4.2 Illustration of changes in QO as defined by equation 4.1 with changing reactant distribution through the reactor

QO can be calculated by solving equations of diffusion (or another process driving micromixing, e.g. differential mobility). The solutions will be functions $R_i(\vec{r})$ defined by initial

distributions of the reactants and the reactor's geometry. These functions are then used in equation 4.1 to calculate *QO*.

4.4 Correlation between the *QO* Parameter and Product Yield

To examine whether or not *QO* correlates with the product yield, we used a system, in which the reaction and diffusion are uncoupled due to different characteristic times of diffusion and reaction. The reactor was a capillary in which reactants were mixed by TDLFP.[96, 101, 105] Due to a very high ratio between the length and the diameter of such a reactor, transverse diffusion establishes concentration profiles of the reactants much faster than longitudinal diffusion. If the characteristic time of reaction is intermediate to those of transverse and longitudinal diffusions, then the reaction and diffusion are uncoupled. Diffusion in the longitudinal direction can be neglected in the time scale of the reaction, and the reaction can be neglected in the time scale of diffusion in the transverse direction. This allowed us to avoid working in meso-scales.[106] The concentration profiles established after TDLFP mixing were used to calculate *QO*, which we then tested for its correlation to the reaction product yield.

The reaction we considered was hybridization of 2 complementary single-strand DNA molecules, R_1 and R_2. The characteristic time of this reaction, τ_{react}, satisfies the following condition[104]:

$$\tau_{trans} << \tau_{react} << \tau_{longit}, \quad \tau_{trans} \equiv r^2/D, \quad \tau_{longit} \equiv L^2/D \qquad 4.2$$

Here, τ_{trans} and τ_{longit} are characteristic times of diffusion in transverse and longitudinal directions, r is the inner radius of the capillary, L is the length of the injected reactant plugs, and D is the diffusion coefficient. For example, $\tau_{trans} = 6$ s and $\tau_{longit} = 10^6$ s for typical parameters of

r = 25 μm, L = 1 cm, and D = 10^{-6} cm^2/s. Different degrees of TDLFP-based mixing were achieved by varying: (i) inner capillary diameter, (ii) pressure used for injection of R_1 and R_2, and (iii) duration of pressure pulses as shown in **Table 4.1**.

The after-mixing profiles of linear concentrations, $R_1(x)$ and $R_2(x)$, where x is the distance from the capillary inlet, were calculated for 6 sets of experimental parameters, using an approach described elsewhere[107] and are shown in **Figure 4.3**. The values of QO were calculated using these profiles and equation 4.1 and are also shown in **Figure 4.3**. The reactor's volume was defined as a volume where at least one reactant is present. The next goal was to find product yields for different degrees of mixing.

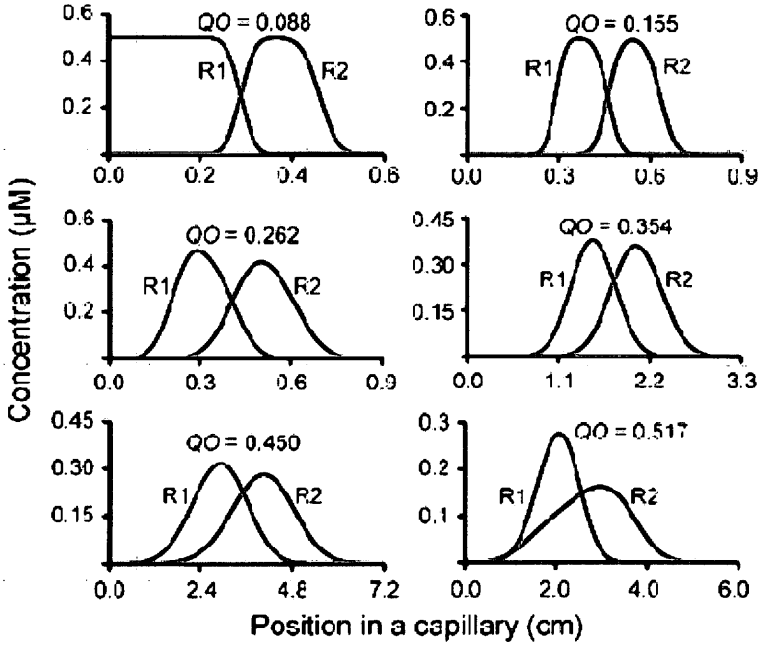

Figure 4.3 Calculated concentration profiles of two reactants, R_1 and R_2, after mixing inside a capillary by TDLFP. The corresponding values of QO are shown inside the panels. Capillary diameters, as well as reactant orders, pressures, and times used for the calculations (and experimental injections) are shown in Table 4.1

To determine the yield of the hybridization reaction product, P, we fluorescently labeled reactant R_1 so that P was also labeled. After TDLFP-based mixing of R_1 and R_2, the reaction was allowed to proceed to completion, and P was separated from the unreacted R_1 by capillary electrophoresis (see **Figure 4.4**).

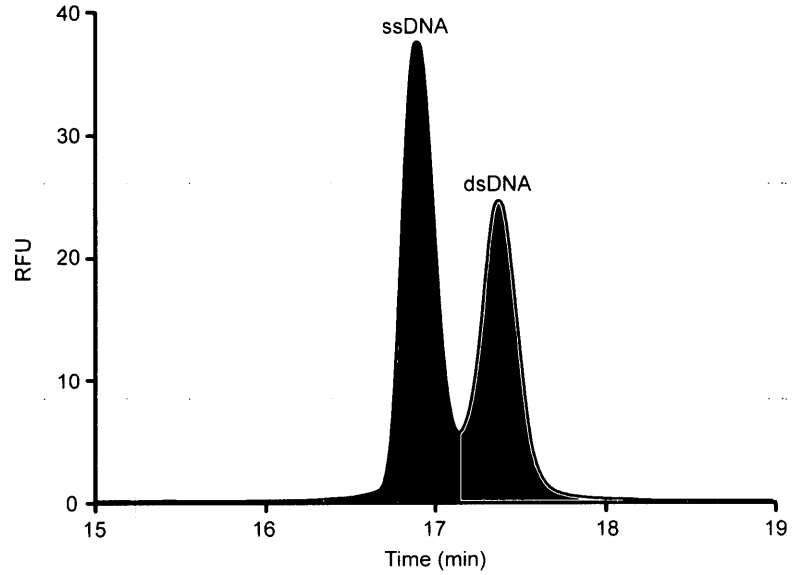

Figure 4.4 Electrophoretic separation of ssDNA (blue area) from dsDNA (red area)

Peak areas in capillary electrophoresis are proportional to amounts of corresponding analytes. Therefore, the yield of P relative to the amount of injected R_1 was calculated as $A_{red}/(A_{red} + A_{blue})$, where A_{red} and A_{blue} are peak areas corresponding to P and unreacted R_1, respectively. The product yield was determined for all of the mixing scenarios shown in **Figure 4.3**. The experiments were done in triplicates. By plotting the experimentally-determined relative product yield versus the theoretically calculated QO, we found that, remarkably, the two parameters linearly correlate, with an intercept very close to 0 and a slope of approximately 1 (**Figure 4.5**).

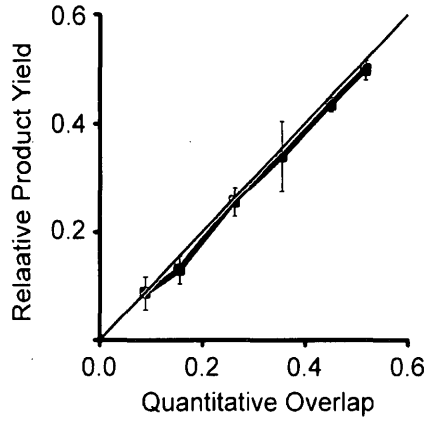

Figure 4.5 Dependence of product yield on QO. See the text for details

4.5 Conclusions

This correlation between *QO* and the product yield is not circumstantial. *QO* is based on the minimum of the normalized reactant concentrations in any given point of the reactor (see Equation 4.1). If the amounts of all reactants in the reactor (defined by denominators in Equation 4.1) are similar, then this minimum identifies the reactant in deficiency in every point, and *QO* can be approximately calculated as an integral of this reactant concentration divided by *A*, where *A* is the amount of one of the reactants. The choice of such a reactant cannot significantly affect *QO* since all the reactant amounts are similar.[104] On the other hand, the local product yield cannot exceed the amount of the reactant in deficiency in every point. As a result, the ratio of total product yield to the amount *A* (i.e. relative yield) should be approximately proportional to *QO* if the reaction proceeds to completion almost everywhere in the reactor.

It should be noted that the choice the experimental example, a capillary with sequentially injected reactants, is only a matter of convenience. *QO* is applicable to different geometries of microreactors and different scenarios of micromixing. It is applicable, in particular, to continuous-flow microreactors, which are widely used by synthetic chemists.[85-95] We introduce

QO, the first predictive quantitative measure to characterize the degree of micromixing. We experimentally prove that *QO* is predictive of relative product yield by using an example of a bimolecular reaction in a capillary microreactor. The generality of the parameter makes it applicable to different types of reactions and reactors as long as micromixing is a sole means of mixing. *QO* can be used to optimize micromixing for maximum product yield by simply maximizing a single easily calculated parameter (a goal that has, so far, remained very difficult to achieve). Other predictive quantitative measures of micromixing can be designed to serve varying needs.

4.6 Materials and Methods

4.6.1 Materials

The HPLC-purified, fluorescently-labeled 15-mer DNA (5'-Alexa488-GCG GAG CGT GGC AGG), and complimentary 15-nucleotide DNA (5'-CCT GCC ACG CTC CGC) were purchased from IDT DNA Technology Inc. (Coralville, IA, USA) and dissolved in a TE buffer (10 mM Tris-HCl, 0.1 mM EDTA, pH 7.5) to have 100 μM stock solutions that were stored at -20 °C. All other chemicals were purchased from Sigma-Aldrich (Oakville, ON, Canada). Uncoated fused-silica capillaries with 75, 50, and 20 μm inner diameters (375 μm outer diameter) were purchased from Polymicro (Phoenix, AZ, USA). The capillary was mounted on a capillary electrophoresis (CE) instrument (P/ACE MDQ, Beckman Coulter, Fullerton, CA, USA), which was equipped with temperature-controlled sample storage and thermal control of the capillary. All solutions were made using deionized water filtered through a 0.22 μm filter (Millipore, Nepean, ON, Canada).

4.6.2 Instrument Modifications

To accurately record pressure profiles, the CE instrument was modified with a commercially-available pressure transducer (MadgeTech PRTrans1000IS Pressure Data Logger). The transducer was attached to the pressure line that feeds the pressure to the capillary inlet. To protect the transducer from excessive pressure, a pressure valve was installed upstream of the transducer. The valve was controlled by a pressure sensor that was set up to close the valve once the pressure was higher than a selected threshold value. The transducer was recording the injection pressure as a function of time and the obtained data was downloaded from the transducer via a USB cable onto a computer using the software provided with the transducer.

4.6.3 Experimental Procedure

The DNA working solutions were prepared separately at a concentration of 500 nM in 100 mM TES buffer pH 7.5. The prepared solutions were injected into a 50-cm capillary, using parameters outlined in **Table 4.1.** The injected reactants were incubated in the capillary at room temperature for 1 min to facilitate formation of dsDNA hybrid. The separation in 100 mM TES buffer pH 7.5 was then performed as outlined in **Table 4.1**. The separation modes were different to prevent overheating of the capillary and DNA hybrid dissociation.

Table 4.1 Experimental parameters used for TDLFP-based mixing of two reactants and their calculated post mixing concentration profiles

	Mixing Scenario	Final Reactants Distribution
1	Capillary Diameter: 20 µm Injection Sequence: 1) DNA B: 1 psi × 15 s 2) DNA A: 1 psi × 25 s Separation : 30 kV, 15 min	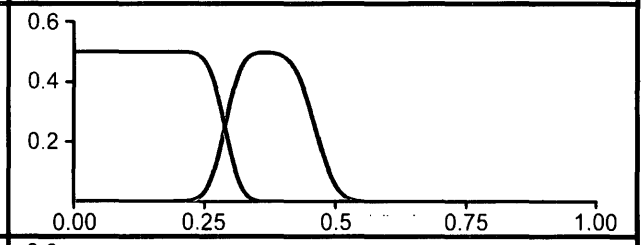
2	Capillary Diameter: 20 µm Injection Sequence: 1) DNA B: 1 psi × 15 s 2) DNA A: 1 psi × 15 s 3) Buffer: 1 psi × 25 s Separation: 30 kV, 15 min	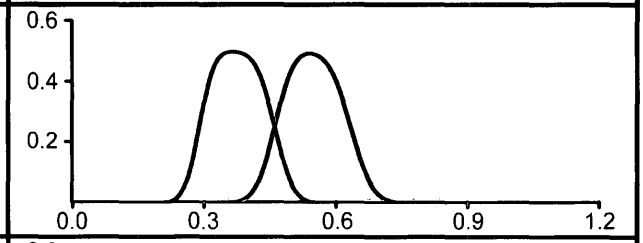
3	Capillary Diameter: 50 µm Injection Sequence: 1) DNA B: 0.5 psi × 15 s 2) DNA A: 0.5 psi × 15 s 3) Buffer: 0.5 psi × 15 s Separation: 1) 10 kV, 10 min 2) 30 kV, 10 min	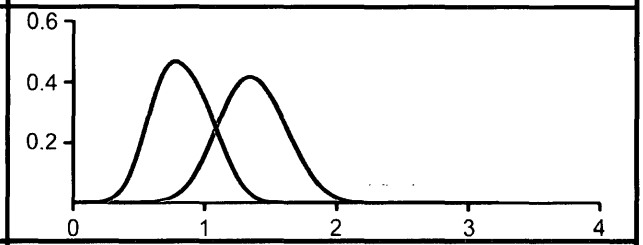
4	Capillary Diameter: 50 µm Injection Sequence: 1) DNA B: 0.5 psi × 15 s 2) DNA A: 0.5 psi × 14 s 3) Buffer: 0.5 psi × 35 s Separation: 1) 10 kV, 10 min 2) 30 kV, 10 min	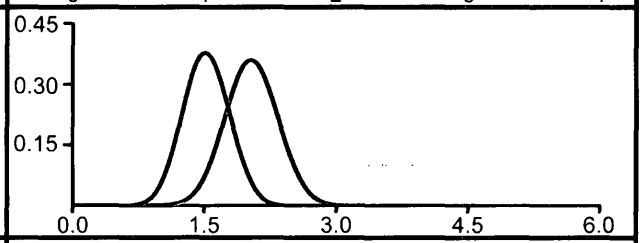
5	Capillary Diameter: 75 µm Injection Sequence: 1) DNA B: 0.3 psi × 14 s 2) DNA A: 0.3 psi × 14 s 3) Buffer: 0.3 psi × 28 s Separation: 1) 7.5 kV, 10 min 2) 20 kV, 15 min	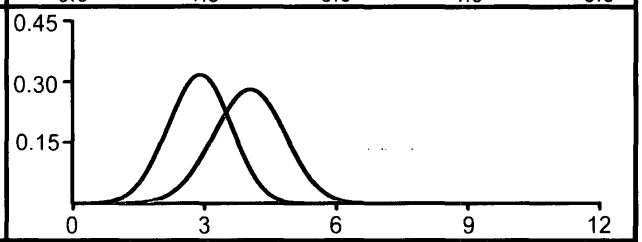
6	Capillary Diameter: 75 µm Injection Sequence: 1) DNA B: 0.3 psi × 14 s 2) DNA A: 0.3 psi × 13 s 3) Buffer: 0.3 psi × 35 s Separation: 1) 7.5 kV, 10 min 2) 20 kV, 15 min	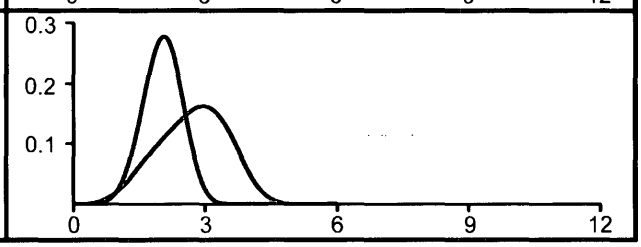

Chapter 5. Separation-based approach to study dissociation kinetics of non-covalent DNA-multiple protein complexes

The presented material was published previously. Adapted with permission from **Petrov, A. P.**; Cherney, L. T.; Dodgson, B.; Okhonin, V.; Krylov, S. N., Separation-Based Approach to Study Dissociation Kinetics of Noncovalent DNA-Multiple Protein Complexes. *J Am Chem Soc* **2011,** *133* (32), 12486-12492.

Contribution to the article: performed all experiments, participated in data analysis, prepared some of the figures, participated in manuscript writing

5.1 Introduction

Non-covalent binding of a single DNA molecule with multiple proteins is common in biology and plays a pivotal role in regulation of gene expression, DNA replication, DNA integrity control, and virus replication.[70, 108] In order to understand the dynamics of these fundamental biological processes, it is important to know kinetic parameters for all steps involved in the formation and dissociation of the relevant DNA-multiple protein complexes.[109-111] Proteins in these complexes can be bound to the DNA directly or indirectly through other proteins. Our knowledge of DNA-multiple protein complexes is typically limited to the identities of the DNA and proteins involved.[112] Complete kinetic analyses are rarely performed for DNA interaction with a single protein[113] and, to the best of our knowledge, kinetics of formation and/or dissociation of DNA-multiple protein complexes have never been measured. The lack of comprehensive kinetic studies is solely due to a lack of experimental approaches capable of distinguishing kinetics of the multiple interconnected processes involved in assembly/disassembly of DNA-multiple protein complexes. The present work was motivated by the insight that, in general, the kinetics of processes occurring during the formation and/or dissociation of DNA-multiple proteins complexes *in vitro* can be distinguished if different complexes move with different velocities, or, in other words, are continuously spatially

separated. Here we present the first separation-based approach for studying kinetics of dissociation of DNA-multiple protein complexes.

In general, to study the dissociation kinetics of DNA-multiple protein complexes, the following 2-step operation should be performed. In the first step (equilibration step), multiple DNA-protein complexes are formed by incubating free DNA with proteins, ideally, long enough to approach equilibrium. In the second step (dissociation step), unbound proteins are continuously removed from the complexes so that the rates of complex formation become zero and the complexes are forced to dissociate. The difficulty of analyzing dissociation kinetics originates from multiple kinetic processes (i) occurring simultaneously and (ii) being indistinguishable from the detection standpoint. When dissociation is initiated by removing free proteins, all DNA-protein complexes start dissociating simultaneously, which results in multiple overlapping single-exponential kinetic curves of the same nature. The resulting signal is the sum of all individual kinetics as conceptually shown in **Figure 5.1, left**. It is a well known problem that the sum of single-exponential curves has a shape close to exponential and in many cases such a sum cannot be used to reliably determine powers of individual exponents comprising it.[35] Errors can become unacceptably large if some components have close (or very different) powers and/or intensities, and if the number of components is unknown (in the other words, the mechanism of reaction is unknown).[35]

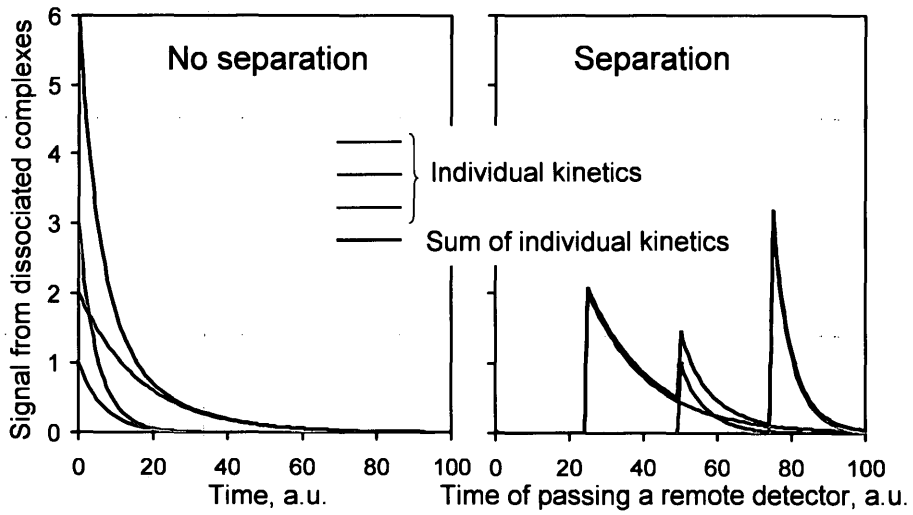

Figure 5.1 Schematic illustration of simultaneous dissociation kinetics of DNA-multiple protein complexes without separation (left) and with separation of the complexes. In each panel, three colour traces show three individual single-exponential kinetics, and a black trace shows their sum

The present work was motivated by the idea that the problem of resolving individual kinetics could be solved by simply making different complexes move with different velocities in the same direction and by placing a detector at a distance x from the site of initiation of movement. Single-exponential curves generated at the detection point by the dissociation of complexes moving with different velocities would be shifted with respect to each other as conceptually shown in **Figure 5.1, right**. It is clear that the sum of such shifted kinetics is more "informative" about its components than the sum of the non-shifted kinetics. It is not clear, however, whether or not this gain can be utilized for the determination of rate constants and for testing hypothetical mechanisms of dissociation. To answer this question, in this proof-of-principle work, we used extensive computer simulation to compare no-separation and separation-based approaches. We examined our method's ability to test hypothetical mechanisms of dissociation. We then demonstrated experimental use of our approach in the study of dissociation

kinetics of complexes of DNA with multiple molecules of the single-stranded DNA-binding protein.[114] As a practical means of introducing differential mobilities of different DNA-protein complexes we used capillary electrophoresis (CE).[46] CE simply provides an efficient way to accomplish the separation-based analysis of simultaneous dissociation processes of DNA-multiple proteins complexes. Our separation approach can potentially be used to study the disassembly kinetics of complex protein machines attached to DNA. We foresee that a separation approach will be also developed to study the kinetics of the formation of DNA-multiple protein complexes.

5.2 Mathematical Model

Our goal is to compare the proposed separation-based approach with the no-separation approach in studying dissociation kinetics of DNA-multiple protein complexes. We first specify the difference between the no-separation and separation approaches. In the no-separation approach, all complexes are spatially co-located and dissociation is detected due to "mass-loss" upon the dissociated components' leaving the point of localization. Sensor-based methods, such as surface plasmon resonance (SPR),[36] fall in the category of the no-separation approach. To study dissociation of DNA-multiple protein complexes with SPR, one would immobilize DNA on the surface and form different complexes on the surface by adding proteins in solution. Dissociation would be initiated and maintained by continuously removing free proteins from the solution and observing mass loss on the surface due to proteins leaving the surface. The resulting signal is a sum of non-shifted exponential curves similar to those depicted in **Figure. 5.1, left**.

The separation approach is based on: (i) continuous spatial separation of different DNA-multiple protein complexes in solution by introducing their differential mobility in one direction,

(ii) dissociation of complexes during their separation, and (iii) following spatial distribution of DNA. While differential mobility can be caused by different means, electrophoresis is the most practical and best-developed way of mobility shift for DNA-protein complexes. The resulting signal will be conceptually similar to spatially shifted exponential curves depicted in **Figure 5.1, right**.

The major disassembly mechanism considered in this work was sequential dissociation from the state of equilibrium (we also considered branched dissociation from the state of equilibrium; **Mechanism 3**). In the first step, N DNA-protein complexes (DP_1, ..., $DP_1...P_N$) are formed by incubating free DNA (D) with N proteins (P_1, ... P_N), ideally, long enough to approach equilibrium:

$$D \underset{}{\overset{P_1, K_{d,1}}{\rightleftharpoons}} DP_1 \overset{P_2, K_{d,2}}{\rightleftharpoons} DP_1P_2 \quad ... \quad \overset{P_N, K_{d,N}}{\rightleftharpoons} DP_1P_2...P_N \qquad 5.1$$

where $K_{d,1}$, $K_{d,2}$, ... $K_{d,N}$ are equilibrium dissociation constants of N sequential processes and the index also denotes the reverse order of dissociation (see Equation 5.2 below). If all proteins are the same, indexes 1, 2, ... N can be omitted as it is done in **Mechanisms 1** and **2** below. In the second step, unbound proteins are continuously removed from the complexes so that the rates of the forward processes in Reaction 5.1 become zero and the complexes are forced to dissociate:

$$DP_1P_2...P_N \xrightarrow{k_{off,N}} DP_1P_2P_{N-1} \xrightarrow{k_{off,N-1}} \quad ... \quad DP_1 \xrightarrow{k_{off,1}} D \qquad 5.2$$

where $k_{off,N}$, $k_{off,N-1}$, ... $k_{off,1}$ are dissociation rate constants for the N DNA-protein complexes. The exact mechanism of complex assembly was not a subject of investigation in this work. Therefore, the sole purpose of equilibrium Reaction 5.1 was to define the initial concentrations

of complexes before dissociation. Reaction 5.2 was instead our major concern and it was investigated using a system of differential equations. To write such a system we define the following terms for complexes:

$$C_0 = D,\ C_1 = DP_1,\ C_2 = DP_1P_2,\ \ldots,\ C_N = DP_1P_2\ldots P_N, \tag{5.3}$$

Then, the no-separation approach is described by a system of ordinary differential equations:

$$\begin{aligned} &d_t C_N = -k_{\text{off},N} C_N, \\ &d_t C_{N-1} = k_{\text{off},N} C_N - k_{\text{off},N-1} C_{N-1} \\ &\ldots \\ &d_t C_1 = k_{\text{off},2} C_2 - k_{\text{off},1} C_1 \\ &d_t C_0 = k_{\text{off},1} C_1 \end{aligned} \tag{5.4}$$

The separation-based approach is described by a system of partial differential equations:

$$\begin{aligned} &\partial_t C_N + v_N \partial_x C_N = -k_{\text{off},N} C_N \\ &\partial_t C_{N-1} + v_{N-1} \partial_x C_{N-1} = k_{\text{off},N} C_N - k_{\text{off},N-1} C_{N-1} \\ &\ldots \\ &\partial_t C_1 + v_1 \partial_x C_1 = k_{\text{off},2} C_2 - k_{\text{off},1} C_1 \\ &\partial_t C_0 + v_0 \partial_x C_0 = k_{\text{off},1} C_1 \end{aligned} \tag{5.5}$$

In equations 5.4 and 5.5, C_n and v_n are a concentration and a migration velocity of a complex with n proteins ($0 \le n \le N$), respectively; d_t is ordinary derivation by time t; ∂_t and ∂_x are partial derivations by time t and spatial coordinate x, respectively. It is easy to see that Equation 5.4 is a degenerate case of equation 5.5 when all velocities are equal to zero.

N equations in 5.4 and 5.5 describe N independent pathways of sequential multi-stage dissociations of N complexes. For example, if DNA can bind at most three proteins, there are

three complexes (plus unbound DNA) in the initial mixture produced by Reaction 5.1. Hence, the 3 equations in either system of differential equations describe three independent pathways starting at $N = 3$, 2, and 1, respectively.

The solution for equations 5.5 and 5.4 can be found by an approach described elsewhere.[35] By using the found solutions of 5.4 and 5.5 we simulated a sum of kinetic traces (also called simulated experimental traces) for the no-separation and separation approaches for two hypothetical mechanisms of disassembly. We also added noise to the simulated experimental traces to mimic real experimental data. We then fit simulated experimental traces with model traces by varying rate constants and amounts of initial complexes using the method of least squares that minimizes the sum of squared differences between the model and simulated experimental traces.[115] Non-linear regression was utilized to obtain the best fit. The rate constants and amounts of initial complexes that led to the best fit were considered the sought ones. The comparison of fundamental properties of the no-separation and separation approaches requires that only fundamental processes (dissociation and migration) are considered. Hence, no other processes (e.g. diffusion, convection, interaction with reactor walls, etc.) were taken into account when building simulated experimental traces for either approach. Accordingly, no additional processes were taken into account when building the model traces used to fit the simulated experimental traces.

5.3 Comparison of No-Separation and Separation Approaches

Figure 5.2 shows an example of a comparison between the no-separation and separation approaches for a reaction mechanism in which one DNA molecule (D) sequentially binds up to three molecules of the same protein (P):

$$D \underset{}{\overset{P,K_{d,1}}{\rightleftharpoons}} DP \underset{}{\overset{P,K_{d,2}}{\rightleftharpoons}} DPP \underset{}{\overset{P,K_{d,3}}{\rightleftharpoons}} DPPP$$

$$DPPP \xrightarrow{k_{off,3}} DPP \xrightarrow{k_{off,2}} DP \xrightarrow{k_{off,1}} D \qquad \text{(Mechanism 1)}$$

Velocities of DPPP, DPP, DP, and D in the separation-based approach were chosen to be: $v_{DPPP} = 0.32$, $v_{DPP} = 0.28$, $v_{DP} = 0.17$, and $v_D = 0.12$. **Figure 5.2** shows simulated experimental and model traces for this mechanism of dissociation. Note that the units are not essential in numerical experiments. Good-quality fitting could be obtained for both no-separation and separation approaches. However, the no-separation approach resulted in good fitting when the errors in rate constant determination were very large (upper table in **Figure 5.2**). Indeed, only the rate constant of the slowest process was found accurately. The other two rate constants were determined with poor accuracy. The no-separation approach also led to large errors in initial concentrations of the complexes (see **Table 5.1**). In contrast, the separation approach determined all three rate constants with high accuracy (lower table in **Figure 5.2**) even though the level of computer-generated random noise was setup at a much higher level. The separation approach also accurately determined the initial concentrations of the complexes (see **Table 5.1**). It is instructive to compare the imaginary separation-based trace in **Figure 5.1** with the simulated separation-based trace in **Figure 5.2**.

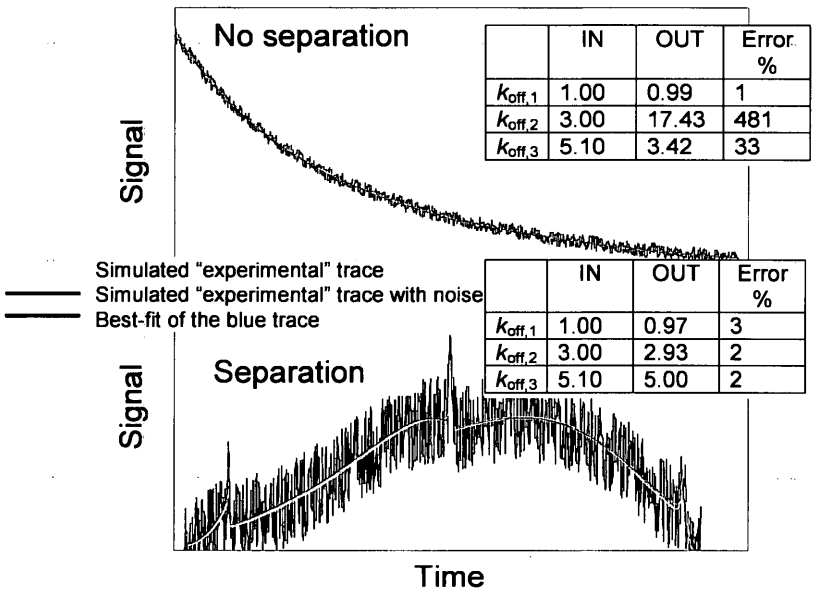

	IN	OUT	Error %
$k_{off,1}$	1.00	0.99	1
$k_{off,2}$	3.00	17.43	481
$k_{off,3}$	5.10	3.42	33

	IN	OUT	Error %
$k_{off,1}$	1.00	0.97	3
$k_{off,2}$	3.00	2.93	2
$k_{off,3}$	5.10	5.00	2

Figure 5.2 Numerical illustration of rate constant determination for simultaneous dissociation of three complexes of DNA with the same protein P by no-separation and separation-based approaches. DNA is assumed to be detected. Accordingly, in the "no-separation" approach, the signal is the cumulative concentration of intact DNA-protein complexes. Such a signal would be generated if the dissociation kinetics of DNA-multiple protein complexes was studied by sensor-based techniques, such as surface plasmon resonance (SPR), with DNA immobilized on the sensor. In the separation-based approach, the signal is the concentration of DNA free or within the complexes. The separation trace has a noise level of 30%. The no-separation trace has a noise level of 5%. The tables in the panels show the actual (IN) and determined (OUT) rate constants as well as the deviations of the determined from the actual ones

Due to the interplay between the three processes in dissociation **Mechanism 1**, the simulated trace in **Figure 5.2** does not show explicit exponential regions that one could intuitively expect. The three kinetic processes in **Mechanism 1** sum up into a trace of more complex shape. Numerical approaches are required, in general, for the extraction of kinetic information from such complex kinetic shapes.

Table 5.1 Comparison of the quality of determination of k_{off} and initial concentrations for the no-separation and separation-based approaches. The red color is used to highlight the values of determined parameters that deviate from the values used for simulation by a factor of 2 or more

Parameter	Value used for simulation	Value obtained with no-separation method	Value obtained with separation-based method
$k_{off,1}$	1.00	0.99	0.97
$k_{off,2}$	3.00	17.43	2.94
$k_{off,3}$	5.10	3.42	5.00
$[DPPP]_{ini}$	2.000	1.784	1.155
$[DPPP]_{ini}$	0.500	0.000	0.498
$[DPP]_{ini}$	0.200	1.844	0.243
$[D]_{ini}$	0.0200	Not determined	0.122

The determination of rate constants by any method is very difficult even for known mechanisms. It would be very useful if the same method could also test a hypothetical mechanism for correctness. Therefore, as our next simulation experiment we compared the no-separation and separation approaches in their ability to distinguish between correct and incorrect mechanisms. For this purpose, simulated experimental traces obtained with **Mechanism 1** were used. As an incorrect mechanism we chose the worst-case-scenario mechanism with the same number of complexes and the same migration velocities as in **Mechanism 1**. In this case, the incorrect mechanism cannot be distinguished from the correct one based on a pattern of peaks in the model trace. The incorrect mechanism was the following:

$$D \underset{}{\overset{P,\,K_{d,1}}{\rightleftharpoons}} DP, \quad DP^*P^* \underset{}{\overset{P,\,K_{d,3}}{\rightleftharpoons}} DP^*P^*P$$
$$DP^*P^*P \xrightarrow{k_{off,3}} DP^*P^*, \quad DP \xrightarrow{k_{off,1}} D \qquad \text{(Mechanism 1')}$$

Here, protein molecules P* are assumed to form a very stable complex ($K_d \rightarrow 0$) with DNA; as a result, the P* molecules cannot dissociate from DNA. Even though an incorrect model does not have to be biologically relevant for our test, **Mechanism 1'** may describe a real mechanism in cells when two protein molecules become cross-linked due to a free radical reaction.

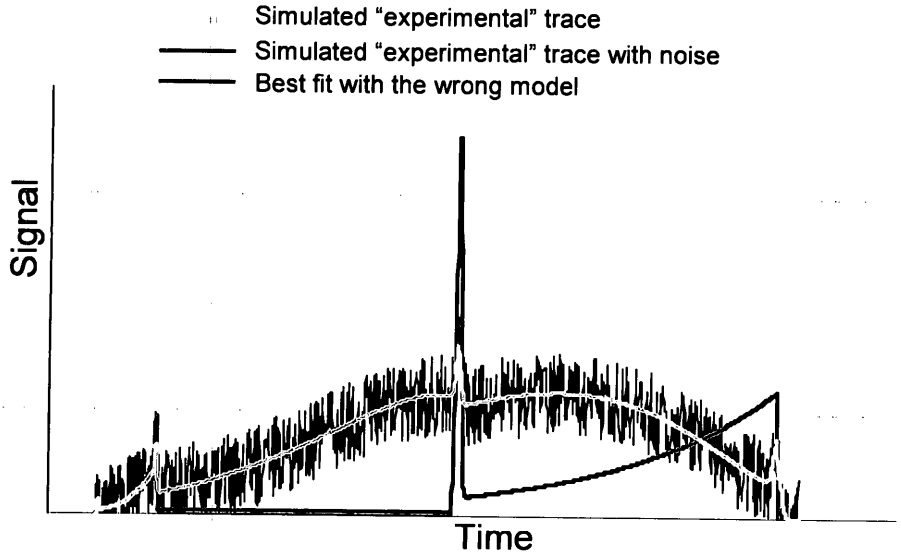

Figure 5.3 Numerical illustration of the best fit with an incorrect model. Simulated signal corresponds to **Mechanism 1** with a noise level of 10% (it is similar to the signal at the bottom of **Figure 5.2**) whereas the model corresponds to **Mechanism 1'**

The result of using the incorrect **Mechanism 1'** for fitting the simulated experimental trace constructed with **Mechanism 1** is shown in **Figure 5.3**. Though the peaks in the model trace perfectly match those in the simulated experimental one, the best fit is strikingly poor and results in a ten-fold increase in the sum-of-least-squares (compare with fitting the same trace with the correct model in **Figure 5.3**).

To confirm that the above example is not unique, we studied a simpler mechanism 2-stage dissociation of the complexes of one DNA with one or two molecules of the same protein:

$$DPP \xrightarrow{k_{off,2}} DP \xrightarrow{k_{off,1}} D \qquad \text{(Mechanism 2)}$$

Velocities of DPP, DP, and D in the separation-based approach were chosen to be: $v_{DPP} = 0.28$, $v_{DP} = 0.17$, and $v_D = 0.12$. The simulated "experimental" traces and the best fits of them are shown in Figure 5.4.

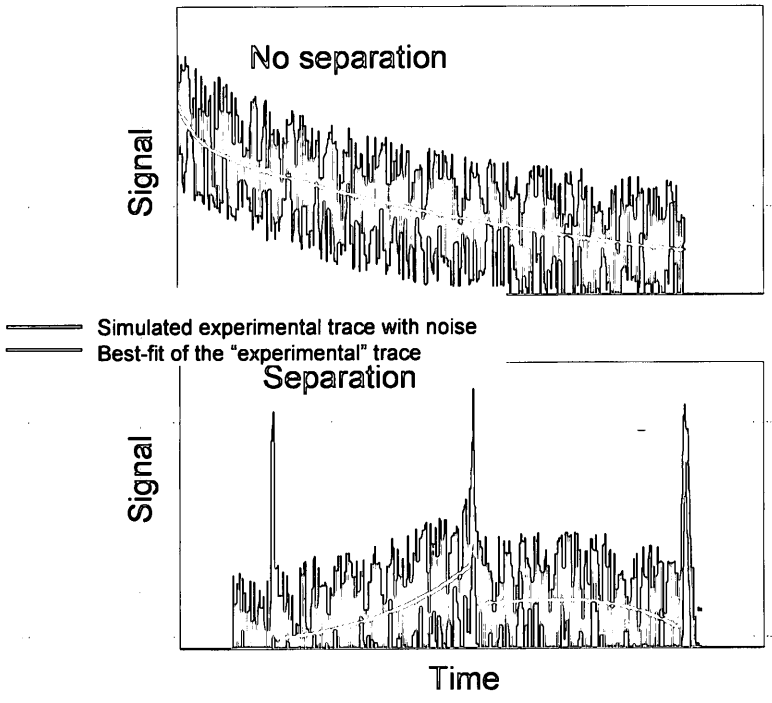

Figure 5.4 Numerical illustration of rate constant determination for simultaneous dissociation of two complexes of DNA with the same protein by no-separation and separation-based approaches. The dissociation process is described by Mechanism 2. Both traces have a noise level of 30%. The parameters used to simulate the "experimental" traces and the determined parameters are assembled in Table 5.2

The parameters used for simulating the "experimental" traces and the determined parameters are shown in Table 5.2. The data show that even for this simple reaction mechanism, the "no-separation" approach failed to determine 3 parameters of 5, while the separation-based approach determined all 5 parameters.

Table 5.2 Comparison of the quality of determination of k_{off} and initial concentrations for the no-separation and separation-based approaches. The red color is used to highlight the values of determined parameters that deviate from the values used for simulation by a factor of 2 or more

Parameter	Value used for simulation	Value obtained with no-separation method	Value obtained with separation-based method
$k_{off,1}$	0.500	0.586	0.567
$k_{off,2}$	2.00	15.97	2.05
$[DPP]_{ini}$	1.000	0.498	1.155
$[DP]_{ini}$	0.130	1.350	0.155
$[D]_{ini}$	0.0800	0.0200	0.0920

As a further test of our method we compared a simulated electropherogram generated by **Mechanism 2** with a model generated by the following mechanism:

$$DP^*P^* \xrightarrow{k_{off,2}} D, \quad DP \xrightarrow{k_{off,1}} D \qquad \text{(Mechanism 2')}$$

Here, as in **Mechanism 1'**, protein molecules P* are P proteins that form a very stable dimer that decays from DNA in one step. The similar charge-to-size ratio of the dimer complex and the two-protein complex of **Mechanism 2** gives equal peak migration times for both mechanisms. However, **Figure 5.5** shows that the model gives a poor fit to the data, as the sum-of-least-squares increases by almost 70% when compared to a fitting that uses the correct mechanism.

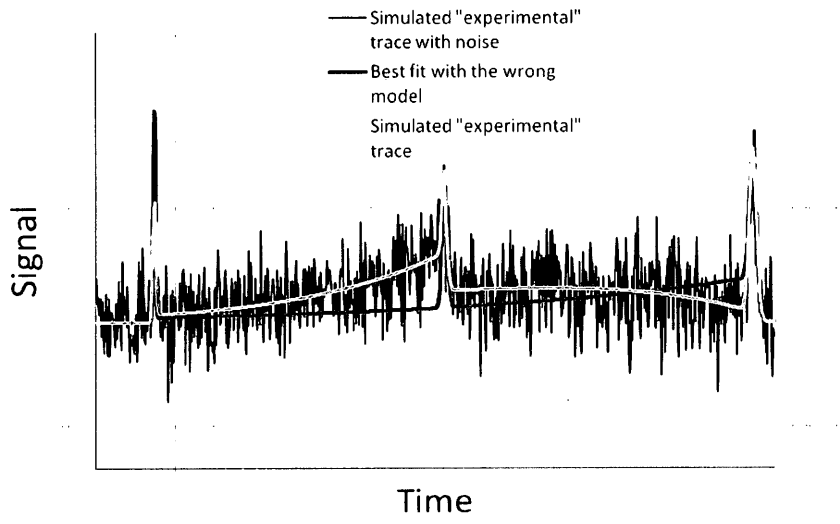

Figure 5.5 Numerical illustration of the best fit with the use of an incorrect model. Simulated signal corresponds to the **Mechanism 2** with a noise level of 10% (it is similar to the signal at the bottom of **Figure 5.4**) whereas the model is given by **Mechanism 2'**

To further test the separation approach we challenged it with a very complex branched mechanism with 16 unknown parameters and 30% noise (see **Mechanism 3)**.

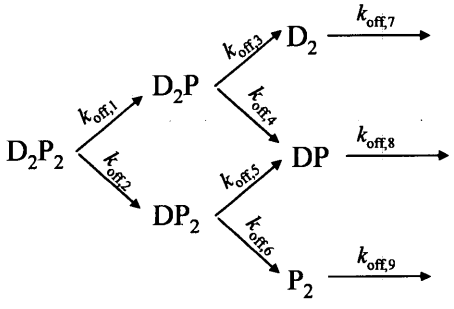

(Mechanism 3)

The velocities of the species in the separation-based approach were arbitrarily chosen to be: $v_{D_2P_2} = 0.28$, $v_{D_2P} = 0.22$, $v_{DP_2} = 0.20$, $v_{DP} = 0.19$, $v_{P_2} = 0.17$, $v_{D_2} = 0.16$, $v_D = 0.18$, and $v_B = 0.12$. Here index 2 denotes the number of molecules of DNA or protein in complexes. We assume that complexes have different charge to size ratios though charge to mass ratios may be the same for D_2P_2 and DP (similarly for D_2 and D). As a result, different velocities were chosen for all

complexes since migration velocities in capillary electrophoresis are determined by charge to size ratios. The simulated "experimental" trace and the best fit of it for the separation-based approach are shown in **Figure 5.6** (the traces for the no-separation approach are similar to those in **Figure 5.4** and not shown).

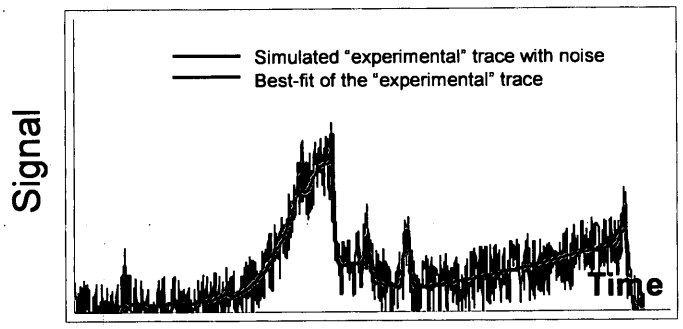

Figure 5.6 Numerical illustration of rate constant determination for simultaneous dissociation of six complexes of DNA with the protein (**Mechanism 3**) by the separation-based approaches. The "experimental" trace has a noise level of 30%. The parameters used to simulate the "experimental" traces and the determined parameters are assembled in **Table 5.3**

The parameters used for simulating the "experimental" traces and the determined parameters are shown in **Table 5.3**. The data show that even for such a complex mechanism, the separation-based approach determined most parameters accurately.

Table 5.3 The quality of determination of k_{off} and initial concentrations for a complex mechanism with 17 parameters by the separation-based approach. The red color is used to highlight the values of determined parameters that deviate from the values used for simulation by a factor of 2 or more

Parameter	Value used for simulation	Value obtained with separation-based method
$k_{off,1}$	3.00	0.304
$k_{off,2}$	2.50	3.53
$k_{off,3}$	1.70	1.33
$k_{off,4}$	2.00	0.82
$k_{off,5}$	2.30	2.27
$k_{off,6}$	1.50	1.11
$k_{off,7}$	0.600	0.619
$k_{off,8}$	1.00	0.96
$k_{off,9}$	0.500	0.431
$[D_2P_2]_{ini}$	1.160	1.202
$[D_2P]_{ini}$	0.140	0.013
$[DP_2]_{ini}$	0.250	0.287
$[DP]_{ini}$	0.015	0.061
$[D_2]_{ini}$	0.050	0.06
$[P_2]_{ini}$	0.090	0.096
$[D]_{ini}$	0.080	0.086
$[P]_{ini}$	0.070	0.095

The separation approach allowed us to accurately determine 8 rate constants out of 9 and 5 initial concentrations out of 7. As any practical approach the separation-based one has its limitations. Accurate determinations of all parameters may be impossible with a single experiment – a number of experiments with different concentrations of proteins may be required for complex mechanisms. Consistent results from the multiple experiments would also ensure that the hypothetical mechanism is correct.

The results allow us to conclude that, in general, the separation approach allows both testing hypothetical mechanisms of dissociation for their feasibility and finding rate constants of dissociation. Thus, the separation approach can be used to create a practical method for studying dissociation kinetics of DNA-multiple protein complexes. In addition, our numerical experiments also confirmed that the mathematical approach used for rate constant determination was also correct and could be reliably applied to rate constant determination from the experimental data even if such data have high level of noise.

5.4 Test of Separation-Based Method in Experiment

To create a practical separation-based method for studying dissociation kinetics of DNA-multiple protein complexes, three technical issues should be addressed. First, different DNA-protein complexes should be separated. Second, free proteins should be continuously removed from the vicinity of the complexes. Third, the concentration of the complexes and free DNA should be measured at a detection point distant from the point of initiation of dissociation. The three conditions can be satisfied by capillary electrophoresis (CE).[61] Due to the high negative charge of DNA, its velocity in gel-free electrophoresis changes significantly upon binding to a protein.[61] Binding to additional proteins should introduce additional changes in velocity. When the equilibrium mixture of DNA and proteins is subjected to an electric field, the DNA-protein complexes are separated from each other and from free proteins. Finally, if DNA is labelled fluorescently, the concentrations of all complexes and free DNA can be measured. We used a commercial CE instrument with fluorescence detection.

As a test experimental model we used the interaction between an 80-nt long single stranded DNA and SSB protein from *E. coli*. SSB proteins bind to single-stranded DNA with

high affinity and are important in DNA replication, recombination, and repair.[116-118] SSB from *E. coli* is composed of four identical subunits and is implicated in DNA metabolism and was shown to stimulate DNA polymerase activity by interacting with it.[7, 116] To facilitate the equilibration step, DNA was mixed with the protein and incubated for 10 min (longer incubation did not influence the results). A short plug of the equilibrated mixture was then injected into the capillary by pressure. To facilitate the dissociation step, a high voltage was then applied to continuously remove free protein from the vicinity of the DNA-protein complexes and to move the complexes with different velocities. DNA was labelled with fluorescein at the 5' end to allow for detection. A single-point detector was used to record an electropherogram with the sum of dissociation kinetics of all complexes. Sometimes the quantum yield of fluorescently-labeled DNA changes upon binding with proteins. This fact can be taken into account by multiplying a modelled concentration of each complex by its corresponding quantum yield. Then, such modelled signals from all complexes are combined to produce a modelled electropherogram that is used in fitting the experimental electropherogram. In the present study we calculated the quantum yields for DPP and DP based on the change in total fluorescence and they were found to be 0.3 and 0.6 respectively. Non-linear regression was used to find the best fit of the experimental electropherogram with a modelled electropherogram (similar to how it was done in the numerical experiments described above). As the protein concentration mixed with DNA was known, the calculations revealed both k_{off} and K_d values.

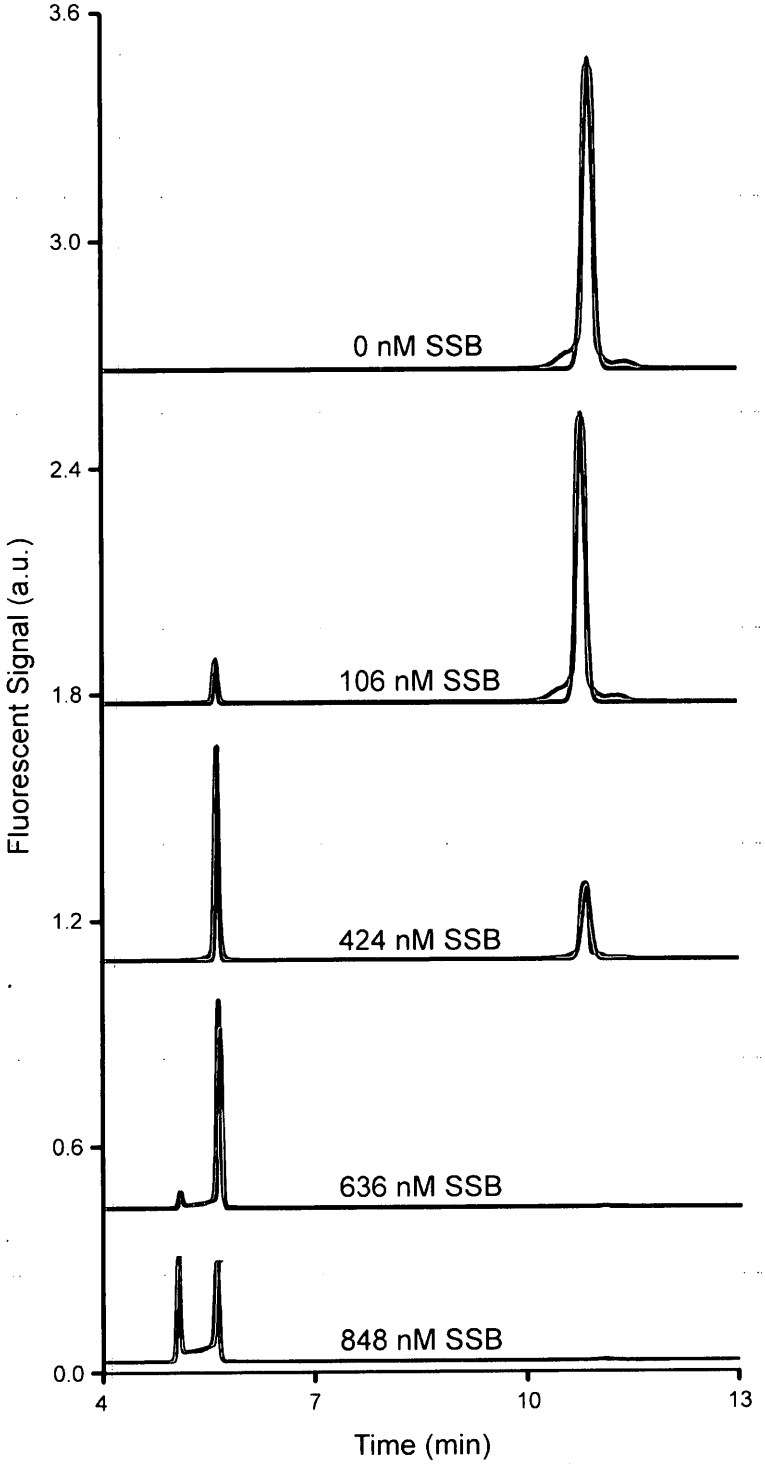

Figure 5.7 Experimental (black lines) and best-fit model (red lines) electropherograms. Experimental electropherograms were obtained for the interaction of fluorescently labeled ssDNA (200 nM) with SSB at varying concentrations. Experimental values of the total protein concentration (including bound and free protein) are shown. The calculated values of the free protein are: 0, 79, 289, 449, and 455 nM, respectively

Figure 5.7 shows representative experimental electropherograms (black traces) for varying concentrations of the protein. The number and combination of peaks in the electropherograms change with changing protein concentration. The right-most peak corresponds to unbound DNA that migrates slower than the complexes. The 2 peaks to the left of it correspond to different DNA-protein complexes. The peak with the shortest migration time is that of the complex with the greatest number of proteins molecules per DNA, which is confirmed by both faster migration time and increase in peak prominence with increasing concentration of the protein. There is pronounced exponential tailing between the left and middle peaks, which suggests that there is significant dissociation of the complex corresponding to left peak. The exponential tailing in **Figure 5.7** is directed from the smaller complex to the larger complex it is formed from. This can be briefly explained in the following way. The highest rate of complex dissociation is in the very beginning, when the concentration of the complex is the highest. A smaller complex (or free DNA), which is generated as a result of the dissociation of a larger complex, will be produced in the largest amount in the very beginning and will migrate close to the peak of the smaller complex (or free DNA). The amount of the smaller complex produced decreases with time while these smaller "portions" will migrate closer to the peak of larger complex. This behavior defines the direction of the tail from the smaller complex to the larger one. There is no detectable tailing between the middle and right peaks even when the dissociation time is increased 10 times by decreasing the electric field strength. This fact indicates that the complex corresponding to middle peak does not dissociate significantly in the time scale of our experiment.

SSB is known to exist in solution predominantly as a tetramer.[116] Depending on conditions (buffer composition, pH, temperature) SSB can bind from 35 to 60 nucleotides per tetramer.[114, 119, 120] The DNA used in the experiments was 80 nucleotides long, so at least two SSB tetramers should theoretically be able to bind to it. Based on this information and on the observation of 2 peaks corresponding to DNA-protein complexes in **Figure 5.7**, we consider the following mechanism for the determination of rate constants:

$$\begin{aligned} &D \underset{}{\overset{P,\,K_{d,1}}{\rightleftharpoons}} DP \overset{P,\,K_{d,2}}{\rightleftharpoons} DPP \\ &DPP \xrightarrow{k_{off,2}} DP \xrightarrow{k_{off,1}} D \end{aligned} \qquad \text{(Mechanism 4)}$$

where P represents a tetrameric protein.

Mechanism 4 does not include peak broadening, as in our particular case the effect of various mechanisms of peak broadening was negligible[35] and, therefore, the model with no peak broadening was used in fitting.

The procedure of building simulated traces was similar to that described above for **Mechanism 1**. The best fits of the experimental data by this model are shown in **Figure 5.7** by red traces. The quality of the fits is high which suggests that **Mechanism 4** satisfactorily describes the experiment. Our calculations returned k_{off} and K_d values shown for convenience in the reaction mechanisms below:

$$\begin{aligned} &D \underset{}{\overset{K_d=102\pm28\text{ nM}}{\rightleftharpoons}} DP \overset{K_d=90\pm57\text{ nM}}{\rightleftharpoons} DPP \\ &DPP \xrightarrow{k_{off,2}=(1.45\pm0.13)\times10^{-3}\,s^{-1}} DP \xrightarrow{k_{off,1}<10^{-4}\,s^{-1}} D \end{aligned} \qquad \text{(Mechanism 4a)}$$

The determined K_d values are in the range of K_d values typically observed for this protein.[121] The detection limit of the instrument and limited time of the experiment did not allow us to accurately measure the k_{off} value for the dissociation of DP; we could only estimate its upper limit. The entire experiment was repeated and the new calculations returned identical values of the constants.

It should be emphasized that we do not claim that **Mechanism 4** of the experimental example is adequately detailed. For instance, DNA can bind a single protein octamer instead of two protein tetramers.[114] Such DNA-protein complexes are identical in their size and charge and cannot be easily distinguished with electrophoresis-based experiments. Thus, the detailed study of complex mechanisms may require a combination of the method suggested here with other techniques.

5.5 Conclusions

To conclude, in this work, we proved in principle that separation-based kinetic methods can facilitate the study of dissociation kinetics of DNA-multiple protein complexes. Separation solves the virtually impossible problem of "extracting" individual single-exponential curves from their sum. Separation can potentially facilitate studying the assembly kinetics of DNA-multiple protein complexes. Further, our approach can be extended to studies of protein-protein interactions if a generic means of separation of multiple-protein complexes is found.

5.6 Materials and Methods

5.6.1 Chemicals, Solutions and Materials

All buffer components were from Sigma-Aldrich (Oakville, ON). All aqueous solutions were made with deionized water and filtered through a 0.22-ím filter (Millipore, Nepean, ON).

SSB protein was from Interscience (Markham, ON, Canada). A fluorescently labelled 80-mer oligonucleotide (5-FAM-CTCCTCTGACTGTAACCACGTGCCTAGCGTTTCATTGTCCCTTCTTATTAGGTGATAA TAGCATAGGTAGTCCAGAAGCC-3) was custom synthesized by IDT Technologies Inc. (Coralwille, IA, USA). The protein and DNA stock solutions as well as equilibrium mixtures were prepared in the incubation buffer (25 mM Borax, pH 10). Fused silica capillaries were purchased from Polymicro (Phoenix, AZ).

5.6.2 Capillary Electrophoresis

CE experiments were performed with a CE instrument (P/ACE MDQ, Beckman-Coulter, USA) with thermo-stabilization of the capillary (the outer walls of the capillary were washed with a liquid heat exchanger maintained at 20°C) and sample vials. The CE method used was Non-Equilibrium Capillary Electrophoresis of Equilibrium Mixtures (NECEEM) .[46] The instrument employed laser-induced fluorescence detection with a 488 nm line of an argon-ion laser for fluorescence excitation. An uncoated fused silica capillary was used with the following dimensions: 50 cm total length/20 μm inner diameter/350 μm outer diameter. The length L from the injection end to the detection window was 40 cm. Electrophoresis was run with a positive electrode at the injection end and an electric field E of 600 V/cm. The run buffer for all NECEEM experiments was the same as the incubation buffer: 25 mM Borax, pH 10. The samples were injected into the capillary by a pressure pulse of 15 s × 2 psi; the length W of corresponding sample plug was ~ 0.6 cm. Prior to each run, the capillary was rinsed with deionized water for 2 min, 100 mM HCl for 2 min, 100 mM NaOH, and, then, the run buffer solution for 2 min. All NECEEM experiments were performed in two repeats.

5.6.3 Equilibrium Mixtures

Equilibrium mixtures of the samples were prepared by mixing the protein and DNA in the incubation buffer and incubating at room temperature for 10 min. The fact that the equilibrium was reached was confirmed by not seeing changes in experimental results for incubation times longer than 10 min. The CE analysis was started immediately after that.

5.6.4 Determination of Experimental Rate and Equilibrium Constants

To determine the rate and equilibrium constants of complex dissociation, experimental electropherograms were fitted with simulated electropherograms obtained using the mathematical model.[35] The model took into account chemical equilibrium at the pre-electrophoresis stage and complex dissociation at the stage of electrophoresis. Minimum mean-square deviation between the experimental and simulated electropherograms was used as a criterion of acceptance of rate constants and equilibrium constant. A computer program, which built simulated electropherograms for varying rate constants and calculated mean-square deviation of the simulated and experimental electropherograms, was written in Excel using Visual Basic and Excel Solver. This program was not optimized for high-speed routine use but was sufficiently productive for the proof-of-principle work.

Limitations

While KCE is a powerful approach to studies of protein-DNA interactions it has a number of limitations. One of the general limitations of KCE, as of an *in vitro* method, is that the obtained kinetics of interactions cannot be transferred to *in vivo* directly. Any *in vitro* experimental system is a simplification, as it deals with a limited set of reacting species, which are freely accessible for reactions. *In vivo* systems are much more complex and interactions observed *in vitro* experiments can occur with different kinetics or may not occur at all. The primary reason for this is the presence of other factors, such as proteins or small molecules in a cell, that are likely to change kinetics of interactions. For example, a DNA element that a protein may readily bind *in vitro*, may not be readily accessible in a cell, as it could be bound by other proteins such as histones. Alternatively, the studied protein may be allosterically regulated and require interactions with other proteins and/or small molecules to bind to the target DNA with high affinity, while in the absence of interacting partners the measured affinity may be quite low, suggesting that the protein is unlikely to bind this particular DNA element. Thus, while *in vitro* methods such as KCE can and should be used to test hypotheses about mechanisms of interactions, they should be based on or verified by data obtained by *in vivo* methods, such as chromatin immunoprecipitation with next generation sequencing.

The major limitation of the KCE approach is the requirement for separation of reacting species. All of the presented methods require separation between reacting species in order to facilitate determination of kinetic constants. While it is possible for simple systems that involve a single protein and DNA, due to significant difference in mobilities, it becomes more challenging for complex systems that involve more than one protein. As the bulkiness of protein-DNA

complexes increase with additional proteins, the mobility of the complex approaches the mobility of the electroosmotic flow, due to increase in the friction coefficient of the complex. This presents a challenge, as it decreases the elution time of the higher order complexes, thus decreasing the separation between them. In such a case the speed of EOF needs to be optimized to allow separation between complexes, which may be challenging.

Concluding Remarks

Most of the previous attempts to study affinity interactions using the separation based methods such as chromatography and electrophoresis assumed an equilibrium during the separation. This assumption is conceptually wrong as it is impossible to physically maintain equilibrium during the separation. Additionally, such an assumption makes it impossible to study and determine the rate constants. However, since the association/dissociation reactions always occur during the separation, the experimental graphs maintain the "memory" of such interactions. Thus we concentrated on defining different ways of how interactions can occur and developing approaches to retrieve kinetic parameters from CE electropherograms. We term this area of research kinetic capillary electrophoresis and define it as CE separation of species that interact during electrophoresis; KCE is not a method but a general concept.

The proposed KCE concept unifies existing kinetic capillary electrophoresis methods and allows a rational design of new kinetic capillary methods tailored to researchers' requirements. KCE methods can be used individually, with the choice of KCE method based on experimenters' needs, as different methods have different accuracies for different kinetic parameters. Alternatively, KCE methods can be used together as an integrated tool - called a multi-method KCE toolbox, which provides a powerful way of testing hypotheses of interactions and accurately calculating binding parameters. One of the major advantages of KCE methods is that some of them can use simplified math for determination of kinetic parameters.

The ppKCE method, introduced in this work, uses the simplified math approach to find both k_{on} and k_{off} constants. Conceptually, in ppKCE the short plugs of reactants are injected into the capillary sequentially; the reactant with lower mobility is injected first. When the voltage is

applied, the faster moving component passes through the slower moving component, resulting in complex formation. The resulting electropherogram has a memory of k_{on} and k_{off}, thus, both constants can be calculated from a single ppKCE electropherogram using areas of peaks and smears and migration times of peaks without nonlinear regression analysis. The ppKCE method is simple and robust, requires only nanoliter volumes of reactants and can be readily adjusted for different ranges of rate constants.

To fully take advantage of the in-capillary mixing method, previously introduced, we developed a predictive parameter to characterize the process of mixing by diffusion. We experimentally proved that the developed parameter is predictive of relative product yield by using an example of a bimolecular reaction, hybridization of two complimentary single-stranded DNA molecules in a capillary. The generality of the parameter makes it applicable to different types of reactions and reactors as long as diffusion is the sole means of mixing. The developed parameter can be used to optimize mixing for maximum product yield by simply maximizing a single easily calculated parameter - a goal that has, so far, remained very difficult to achieve.

As the biologically relevant protein-DNA affinity interactions are typically complex and involve multiple proteins binding to a single DNA molecule, we have applied our developed KCE approach to measure the disassembly kinetics of such complex systems. Our separation-based KCE approach was compared with a conventional no-separation approach by using computer simulation of dissociation kinetics. The KCE approach proved to be much more accurate than the no-separation approach and to be a powerful tool for testing hypothetical mechanisms of the disassembly of DNA-multiple proteins complexes. The interaction between an 80-nucleotide long ssDNA and SSB protein was studied. DNA-protein complexes with one

and two proteins were observed, and rate constants of their dissociation were determined. In this work, we proved in principle that separation-based kinetic methods can facilitate the study of dissociation kinetics of DNA-multiple protein complexes.

In this work we have developed a novel separation-based approach for analysis of protein-DNA affinity interactions. We have demonstrated that separation methods such as CE can be used for studying kinetics of both simple and complex protein-DNA affinity interactions. We foresee that KCE methods will find multiple applications in fundamental studies of biomolecular interactions, designing clinical diagnostics, and the development of affinity probes and drug candidates. New applications will emerge with further development of KCE.

Future Plans

1) The effect of small molecules on protein-DNA interactions.

Small molecules are important effector molecules that can regulate protein-DNA interactions. Regulation by small molecules can be naturally occurring or artificially induced by small molecules selected from combinatorial libraries as drug candidates. In order to understand the mechanism of regulation by small molecules or its pharmacological effect, it is important to measure changes in the kinetic parameters between protein and corresponding DNA molecule that occur when a small molecule is present. KCE methods are a good choice for such comparative studies as both the incubation and separation buffers can be supplemented with a small molecule of interest. In such a case, the difference in kinetic parameters between the experiments with and without the small molecule would indicate the effect of the small molecule as well as the mechanisms of action.

2) Addition of the adsorption/desorption processes to the KCE theory

Protein adsorption/desorption is a relatively common phenomenon in capillary electrophoresis and can significantly contribute to the shape of the experimental graph. In such cases KCE should account for the phenomenon of adsorption/desorption. To understand if the kinetic measurements are possible under such circumstances we need to perform model experiments. A protein exhibiting a significant adsorption to the capillary walls and with previously characterized affinity towards DNA would be used in these model experiments. The adsorption/desorption constants for this particular protein would be determined from a separate set of experiments by propagating the protein through the capillary. The equations describing adsorption/desorption would be included into the KCE system of equations to accommodate the adsorption/desorption phenomenon. The protein-DNA interactions would then be studied using KCE approach, the data would be fitted and the obtained kinetic parameters would be compared with the previously published. Once kinetic constants obtained by KCE would be in agreement with kinetic constants obtained by an alternative method it would indicate that the developed approach correctly accounts for the adsorption phenomenon.

List of Publications

Articles in Refereed Journals

1. Cherney, L.T.; Okhonin, V.; **Petrov, A.P.**; Krylov, S.N. Sequential-dissociation kinetics of a non-covalent complexes of DNA with multiple proteins in separation-based approach: general theory and its application. *Analytica Chimica Acta* **2012**, 724, 111-118.
2. Okhonin, V.; **Petrov, A.P.**; Krylova, S.M.; Krylov, S.N. Quantitative characterization of micromixing based on uniformity and overlap. *Angewandte Chemie International Edition* **2011**, 50, 11999-12002.
3. **Petrov, A.P.**; Cherney, L.T.; Dodgson, B.; Okhonin, V.; Krylov, S.N. Separation-based approach to study dissociation kinetics of non-covalent DNA-multiple protein complexes. *Journal of the American Chemical Society*, **2011**, 133, 12486-12492.
4. **Petrov, A.P.**; Dodgson, B.J.; Cherney, L.T.; Krylov, S.N. Predictive measure of quality of micromixing. *Chemical Communications* **2011**, 47, 7767-7769.
5. Karkhanina, A.A.; Mecinovic, J.; Musheev, M.U.; Krylova, S.M. **Petrov, A.P.**; Hewitson, K.S.; Flashman, E.; Schofield, C.J.; Krylov, S.N. Direct analysis of enzyme-catalyzed DNA demethylation. *Analytical Chemistry* **2009**, 81, 5871-5875.
6. Larijani, M.; **Petrov, A.P.**; Krylov, S.N.; Martin, A. AID is a sequence-independent single-stranded DNA binding protein: preferential mutation of hot-spot motifs is imposed during catalysis. *Molecular and Cellular Biology* **2007**, 27, 20-30.
7. Okhonin, V.; **Petrov, A.**; Berezovski, M.; Krylov, S.N. Plug-plug kinetic capillary electrophoresis: a method for direct determination of rate constants of complex formation and dissociation. *Analytical Chemistry* **2006**, 78, 4803-4810.
8. **Petrov, A.**; Okhonin, V.; Berezovski, M.; Krylov, S.N. Kinetic capillary electrophoresis (KCE): a conceptual platform for kinetic homogeneous affinity methods. *Journal of the American Chemical Society* **2005**, 127, 17104-17110.
9. Berezovski, M.; Drabovich, A.; Krylova, S.M.; Musheev, M.; Okhonin, V.; **Petrov, A.**; Krylov, S.N. Nonequilibrium capillary electrophoresis of equilibrium mixtures: a universal tool for development of aptamers. *Journal of the American Chemical Society* **2005**, 127, 3165-3171.

Papers in Refereed Conference Proceedings

1. Berezovski, M.; Okhonin, V.; **Petrov, A.**; S.N. Krylov. Kinetic methods in capillary electrophoresis and their applications. *Proceeding of the International Society for Optical Engineering* **2005**, 5969, 203-215.

References

1. Luscombe, N. M.; Thornton, J. M., Protein-DNA interactions: Amino acid conservation and the effects of mutations on binding specificity. *J Mol Biol* **2002,** *320* (5), 991-1009.
2. Meyer, R. R.; Laine, P. S., The Single-Stranded DNA-Binding Protein of Escherichia-Coli. *Microbiol Rev* **1990,** *54* (4), 342-380.
3. Witte, G.; Urbanke, C.; Curth, U., DNA polymerase III chi subunit ties single-stranded DNA binding protein to the bacterial replication machinery. *Nucleic Acids Res* **2003,** *31* (15), 4434-4440.
4. Yuzhakov, A.; Kelman, Z.; O'Donnell, M., Trading places on DNA--a three-point switch underlies primer handoff from primase to the replicative DNA polymerase. *Cell* **1999,** *96* (1), 153-63.
5. Lecointe, F.; Serena, C.; Velten, M.; Costes, A.; McGovern, S.; Meile, J. C.; Errington, J.; Ehrlich, S. D.; Noirot, P.; Polard, P., Anticipating chromosomal replication fork arrest: SSB targets repair DNA helicases to active forks. *The EMBO journal* **2007,** *26* (19), 4239-51.
6. Acharya, N.; Varshney, U., Biochemical properties of single-stranded DNA-binding protein from Mycobacterium smegmatis, a fast-growing mycobacterium and its physical and functional interaction with uracil DNA glycosylases. *J Mol Biol* **2002,** *318* (5), 1251-64.
7. Molineux, I. J.; Gefter, M. L., Properties of Escherichia-Coli DNA Binding (Unwinding) Protein - Interaction with DNA-Polymerase and DNA. *P Natl Acad Sci USA* **1974,** *71* (10), 3858-3862.
8. Arad, G.; Hendel, A.; Urbanke, C.; Curth, U.; Livneh, Z., Single-stranded DNA-binding protein recruits DNA polymerase V to primer termini on RecA-coated DNA. *Journal of Biological Chemistry* **2008,** *283* (13), 8274-8282.
9. Geertz, M.; Maerkl, S. J., Experimental strategies for studying transcription factor-DNA binding specificities. *Brief Funct Genomics* **2010,** *9* (5-6), 362-73.
10. Latchman, D. S., *Gene regulation : a eukaryotic perspective*. 5th ed.; Taylor & Francis: New York, 2005; p x, 374 p.
11. Cantin, G. T.; Stevens, J. L.; Berk, A. J., Activation domain-mediator interactions promote transcription preinitiation complex assembly on promoter DNA. *P Natl Acad Sci USA* **2003,** *100* (21), 12003-12008.
12. Kadonaga, J. T., Regulation of RNA polymerase II transcription by sequence-specific DNA binding factors. *Cell* **2004,** *116* (2), 247-257.
13. Yankulov, K.; Blau, J.; Purton, T.; Roberts, S.; Bentley, D. L., Transcriptional Elongation by Rna-Polymerase-Ii Is Stimulated by Transactivators. *Cell* **1994,** *77* (5), 749-759.
14. Blau, J.; Xiao, H.; McCracken, S.; OHare, P.; Greenblatt, J.; Bentley, D., Three functional classes of transcriptional activation domains. *Mol Cell Biol* **1996,** *16* (5), 2044-2055.
15. Kageyama, R.; Pastan, I., Molecular-Cloning and Characterization of a Human DNA-Binding Factor That Represses Transcription. *Cell* **1989,** *59* (5), 815-825.
16. Liu, Y. H.; Yang, N. Y.; Teng, C. T., Coup-Tf Acts as a Competitive Repressor for Estrogen Receptor-Mediated Activation of the Mouse Lactoferrin Gene. *Mol Cell Biol* **1993,** *13* (3), 1836-1846.
17. Zhou, Q. J.; Gedrich, R. W.; Engel, D. A., Transcriptional Repression of the C-Fos Gene by Yy1 Is Mediated by a Direct Interaction with Atf/Creb. *J Virol* **1995,** *69* (7), 4323-4330.

18. HannaRose, W.; Hansen, U., Active repression mechanisms of eukaryotic transcription repressors. *Trends Genet* **1996,** *12* (6), 229-234.
19. Takahashi, K.; Yamanaka, S., Induction of pluripotent stem cells from mouse embryonic and adult fibroblast cultures by defined factors. *Cell* **2006,** *126* (4), 663-76.
20. Johnson, D. S.; Mortazavi, A.; Myers, R. M.; Wold, B., Genome-wide mapping of in vivo protein-DNA interactions. *Science* **2007,** *316* (5830), 1497-502.
21. Garner, M. M.; Revzin, A., A gel electrophoresis method for quantifying the binding of proteins to specific DNA regions: application to components of the Escherichia coli lactose operon regulatory system. *Nucleic Acids Res* **1981,** *9* (13), 3047-60.
22. Hellman, L. M.; Fried, M. G., Electrophoretic mobility shift assay (EMSA) for detecting protein-nucleic acid interactions. *Nat Protoc* **2007,** *2* (8), 1849-61.
23. Bassam, B. J.; Caetano-Anolles, G.; Gresshoff, P. M., Fast and sensitive silver staining of DNA in polyacrylamide gels. *Anal Biochem* **1991,** *196* (1), 80-3.
24. Varshavsky, A., Electrophoretic assay for DNA-binding proteins. *Methods Enzymol* **1987,** *151*, 551-65.
25. Fried, M.; Crothers, D. M., Equilibria and kinetics of lac repressor-operator interactions by polyacrylamide gel electrophoresis. *Nucleic Acids Res* **1981,** *9* (23), 6505-25.
26. Fried, M. G.; Liu, G., Molecular sequestration stabilizes CAP-DNA complexes during polyacrylamide gel electrophoresis. *Nucleic Acids Res* **1994,** *22* (23), 5054-9.
27. Fried, M. G.; Bromberg, J. L., Factors that affect the stability of protein-DNA complexes during gel electrophoresis. *Electrophoresis* **1997,** *18* (1), 6-11.
28. Vossen, K. M.; Fried, M. G., Sequestration stabilizes lac repressor-DNA complexes during gel electrophoresis. *Anal Biochem* **1997,** *245* (1), 85-92.
29. Chance, B., The accelerated flow method for rapid reactions. *J Frankl Inst* **1940,** *229*, 455-476.
30. Morelli, B., Kinetic Experiment Using a Spring Powered, Stopped-Flow Apparatus. *J Chem Educ* **1976,** *53* (2), 119-122.
31. Scott, R. A.; Lukehart, C. M., *Applications of physical methods to inorganic and bioinorganic chemistry*. Wiley: Hoboken, NJ, 2007; p xi, 576 p.
32. Gomezhens, A.; Perezbendito, D., The Stopped-Flow Technique in Analytical-Chemistry. *Anal Chim Acta* **1991,** *242* (2), 147-177.
33. Andreeva, I. E.; Szymanski, M. R.; Jezewska, M. J.; Galletto, R.; Bujalowski, W., Dynamics of the ssDNA Recognition by the RepA Hexameric Helicase of Plasmid RSF1010: Analyses Using Fluorescence Stopped-Flow Intensity and Anisotropy Methods. *J Mol Biol* **2009,** *388* (4), 751-775.
34. Fedorova, O. S.; Nevinsky, G. A.; Koval, V. V.; Ischenko, A. A.; Vasilenko, N. L.; Douglas, K. T., Stopped-flow kinetic studies of the interaction between Escherichia coli Fpg protein and DNA substrates. *Biochemistry-Us* **2002,** *41* (5), 1520-1528.
35. Petrov, A. P.; Cherney, L. T.; Dodgson, B.; Okhonin, V.; Krylov, S. N., Separation-Based Approach to Study Dissociation Kinetics of Noncovalent DNA-Multiple Protein Complexes. *J Am Chem Soc* **2011,** *133* (32), 12486-12492.
36. Schasfoort, R. B. M.; Tudos, A. J., *Handbook of surface plasmon resonance*. RSC Pub.: Cambridge, UK, 2008; p xxi, 403 p.
37. Wilson, W. D., Tech.Sight. Analyzing biomolecular interactions. *Science* **2002,** *295* (5562), 2103-5.

38. Henriksson-Peltola, P.; Sehlen, W.; Haggard-Ljungquist, E., Determination of the DNA-binding kinetics of three related but heteroimmune bacteriophage repressors using EMSA and SPR analysis. *Nucleic Acids Res* **2007,** *35* (10), 3181-3191.
39. Lin, K. C.; Wey, M. T.; Kan, L. S.; Shiuan, D., Characterization of the Interactions of Lysozyme with DNA by Surface Plasmon Resonance and Circular Dichroism Spectroscopy. *Appl Biochem Biotech* **2009,** *158* (3), 631-641.
40. Solomun, T.; Sturm, H.; Wellhausen, R.; Seitz, H., Interaction of a single-stranded DNA-binding protein g5p with DNA oligonucleotides immobilised on a gold surface. *Chem Phys Lett* **2012,** *533*, 92-94.
41. Harding, S. E.; Chowdhry, B. Z., *Protein-ligand interactions : hydrodynamics and calorimetry : a practical approach.* Oxford University Press: Oxford ; New York, 2001; p xxiv, 330 p.
42. Majka, J.; Speck, C., Analysis of protein-DNA interactions using surface plasmon resonance. In *Analytics of Protein-DNA Interactions*, Seitz, H., Ed. 2007; Vol. 104, pp 13-36.
43. Levene, M. J.; Korlach, J.; Turner, S. W.; Foquet, M.; Craighead, H. G.; Webb, W. W., Zero-mode waveguides for single-molecule analysis at high concentrations. *Science* **2003,** *299* (5607), 682-686.
44. Uemura, S.; Aitken, C. E.; Korlach, J.; Flusberg, B. A.; Turner, S. W.; Puglisi, J. D., Real-time tRNA transit on single translating ribosomes at codon resolution. *Nature* **2010,** *464* (7291), 1012-U73.
45. Tsai, A.; Petrov, A.; Marshall, R. A.; Korlach, J.; Uemura, S.; Puglisi, J. D., Heterogeneous pathways and timing of factor departure during translation initiation. *Nature* **2012,** *487* (7407), 390-3.
46. Berezovski, M.; Krylov, S. N., Nonequilibrium capillary electrophoresis of equilibrium mixtures--a single experiment reveals equilibrium and kinetic parameters of protein-DNA interactions. *J Am Chem Soc* **2002,** *124* (46), 13674-5.
47. Okhonin, V.; Berezovski, M.; Krylov, S. N., Sweeping capillary electrophoresis: A non-stopped-flow method for measuring bimolecular rate constant of complex formation between protein and DNA. *J Am Chem Soc* **2004,** *126* (23), 7166-7167.
48. Avila, L. Z.; Chu, Y. H.; Blossey, E. C.; Whitesides, G. M., Use of Affinity Capillary Electrophoresis to Determine Kinetic and Equilibrium-Constants for Binding of Arylsulfonamides to Bovine Carbonic-Anhydrase. *J Med Chem* **1993,** *36* (1), 126-133.
49. Okerberg, E. S.; Wu, J. Y.; Zhang, B. H.; Samii, B.; Blackford, K.; Winn, D. T.; Shreder, K. R.; Burbaum, J. J.; Patricelli, M. P., High-resolution functional proteomics by active-site peptide profiling. *P Natl Acad Sci USA* **2005,** *102* (14), 4996-5001.
50. Licitra, E. J.; Liu, J. O., A three-hybrid system for detecting small ligand-protein receptor interactions. *P Natl Acad Sci USA* **1996,** *93* (23), 12817-12821.
51. Tuerk, C.; Gold, L., Systematic Evolution of Ligands by Exponential Enrichment - Rna Ligands to Bacteriophage-T4 DNA-Polymerase. *Science* **1990,** *249* (4968), 505-510.
52. Woodbury, C. P.; Venton, D. L., Methods of screening combinatorial libraries using immobilized or restrained receptors. *J Chromatogr B* **1999,** *725* (1), 113-137.
53. Mitchell, P., A perspective on protein microarrays. *Nat Biotechnol* **2002,** *20* (3), 225-229.
54. Cooper, M. A., Advances in membrane receptor screening and analysis. *J Mol Recognit* **2004,** *17* (4), 286-315.

55. Yang, P.; Whelan, R. J.; Jameson, E. E.; Kurzer, J. H.; Argetsinger, L. S.; Carter-Su, C.; Kabir, A.; Malik, A.; Kennedy, R. T., Capillary electrophoresis and fluorescence anisotropy for quantitative analysis of peptide-protein interactions using JAK2 and SH2-Bbeta as a model system. *Anal Chem* **2005,** *77* (8), 2482-9.
56. Berezovski, M.; Nutiu, R.; Li, Y. F.; Krylov, S. N., Affinity analysis of a protein-aptamer complex using nonequilibrium capillary electrophoresis of equilibrium mixtures. *Anal Chem* **2003,** *75* (6), 1382-1386.
57. Huang, C. C.; Cao, Z. H.; Chang, H. T.; Tan, W. H., Protein-protein interaction studies based on molecular aptamers by affinity capillary electrophoresis. *Anal Chem* **2004,** *76* (23), 6973-6981.
58. Berezovski, M.; Krylov, S. N., Using DNA-binding proteins as an analytical tool. *J Am Chem Soc* **2003,** *125* (44), 13451-13454.
59. Berezovski, M.; Krylov, S. N., Using nonequilibrium capillary electrophoresis of equilibrium mixtures for the determination of temperature in capillary electrophoresis. *Anal Chem* **2004,** *76* (23), 7114-7117.
60. Berezovski, M.; Krylov, S. N., Thermochemistry of protein-DNA interaction studied with temperature-controlled nonequilibrium capillary electrophoresis of equilibrium mixtures. *Anal Chem* **2005,** *77* (5), 1526-1529.
61. Berezovski, M.; Drabovich, A.; Krylova, S. M.; Musheev, M.; Okhonin, V.; Petrov, A.; Krylov, S. N., Nonequilibrium capillary electrophoresis of equilibrium mixtures: A universal tool for development of aptamers. *J Am Chem Soc* **2005,** *127* (9), 3165-3171.
62. Krylov, S. N.; Berezovski, M., Non-equilibrium capillary electrophoresis of equilibrium mixtures--appreciation of kinetics in capillary electrophoresis. *Analyst* **2003,** *128* (6), 571-5.
63. Okhonin, V.; Krylova, S. M.; Krylov, S. N., Nonequilibrium capillary electrophoresis of equilibrium mixtures, mathematical model. *Anal Chem* **2004,** *76* (5), 1507-1512.
64. Ferrari, M. E.; Bujalowski, W.; Lohman, T. M., Co-operative binding of Escherichia coli SSB tetramers to single-stranded DNA in the (SSB)35 binding mode. *J Mol Biol* **1994,** *236* (1), 106-23.
65. Marcovitz, A.; Levy, Y., Frustration in protein-DNA binding influences conformational switching and target search kinetics. *P Natl Acad Sci USA* **2011,** *108* (44), 17957-62.
66. Hagmar, P.; Dahlman, K.; Takahashi, M.; Carstedt-Duke, J.; Gustafsson, J.; Norden, B., Unspecific DNA binding of the DNA binding domain of the glucocorticoid receptor studied with flow linear dichroism. *FEBS Lett* **1989,** *253* (1-2), 28-32.
67. Shamoo, Y., Single-stranded DNA-binding Proteins. In *eLS*, John Wiley & Sons, Ltd: 2001.
68. Chu, Y. H.; Avila, L. Z.; Biebuyck, H. A.; Whitesides, G. M., Use of Affinity Capillary Electrophoresis to Measure Binding Constants of Ligands to Proteins. *J Med Chem* **1992,** *35* (15), 2915-2917.
69. Heegaard, N. H. H.; Nissen, M. H.; Chen, D. D. Y., Applications of on-line weak affinity interactions in free solution capillary electrophoresis. *Electrophoresis* **2002,** *23* (6), 815-822.
70. Saiz, L.; Vilar, J. M. G., Protein-protein/DNA interaction networks: versatile macromolecular structures for the control of gene expression. *Iet Syst Biol* **2008,** *2* (5), 247-255.
71. Davis, S. J.; Davies, E. A.; Tucknott, M. G.; Jones, E. Y.; van der Merwe, P. A., The role of charged residues mediating low affinity protein-protein recognition at the cell surface by CD2. *P Natl Acad Sci USA* **1998,** *95* (10), 5490-5494.

72. Iakoucheva, L. M.; Walker, R. K.; van Houten, B.; Ackerman, E. J., Equilibrium and stop-flow kinetic studies of fluorescently labeled DNA substrates with DNA repair proteins XPA and replication protein A. *Biochemistry-Us* **2002,** *41* (1), 131-143.
73. Newman-Tancredi, A.; Assie, M. B.; Leduc, N.; Ormiere, A. M.; Danty, N.; Cosi, C., Novel antipsychotics activate recombinant human and native rat serotonin 5-HT1A receptors: affinity, efficacy and potential implications for treatment of schizophrenia. *Int J Neuropsychoph* **2005,** *8* (3), 341-356.
74. Yu, D. H.; Blankert, B.; Vire, J. C.; Kauffmann, J. M., Biosensors in drug discovery and drug analysis. *Anal Lett* **2005,** *38* (11), 1687-1701.
75. Okhonin, V.; Petrov, A. P.; Berezovski, M.; Krylov, S. N., Plug-plug kinetic capillary electrophoresis: method for direct determination of rate constants of complex formation and dissociation. *Anal Chem* **2006,** *78* (14), 4803-10.
76. Petrov, A.; Okhonin, V.; Berezovski, M.; Krylov, S. N., Kinetic capillary electrophoresis (KCE): a conceptual platform for kinetic homogeneous affinity methods. *J Am Chem Soc* **2005,** *127* (48), 17104-10.
77. LeCaptain, D. J.; Michel, M. A.; Van Orden, A., Characterization of DNA-protein complexes by capillary electrophoresis-single molecule fluorescence correlation spectroscopy. *Analyst* **2001,** *126* (8), 1279-1284.
78. Fisher, R. J.; Fivash, M.; Casas-Finet, J.; Bladen, S.; Larson McNitt, K., Real-Time BIAcore Measurements of Escherichia coli Single-Stranded DNA Binding (SSB) Protein to Polydeoxythymidylic Acid Reveal Single-State Kinetics with Steric Cooperativity. *Methods* **1994,** *6* (2), 121-133.
79. Witte, G.; Urbanke, C.; Curth, U., Single-stranded DNA-binding protein of Deinococcus radiodurans: a biophysical characterization. *Nucleic Acids Res* **2005,** *33* (5), 1662-1670.
80. Kozlov, A. G.; Lohman, T. M., Kinetic mechanism of direct transfer of Escherichia coli SSB tetramers between single-stranded DNA molecules. *Biochemistry-Us* **2002,** *41* (39), 11611-11627.
81. Okhonin, V.; Liu, X.; Krylov, S. N., Transverse diffusion of laminar flow profiles to produce capillary nanoreactors. *Anal Chem* **2005,** *77* (18), 5925-5929.
82. Ottino, J. M., *The kinematics of mixing : stretching, chaos, and transport*. Cambridge University Press: Cambridge ; New York, 1989; p xiv, 364 p.
83. Ogawa, K., *Chemical engineering : a new perspective*. 1st ed.; Elsevier: Amsterdam, 2007; p xiv, 175 p.
84. Danckwerts, P. V., The Definition and Measurement of Some Characteristics of Mixtures. *Appl Sci Res* **1952,** *3* (4), 279-296.
85. Pierre, Z. N.; Field, C. R.; Scheeline, A., Sample Handling and Chemical Kinetics in an Acoustically Levitated Drop Microreactor. *Anal Chem* **2009,** *81* (20), 8496-8502.
86. McMullen, J. P.; Jensen, K. F., Integrated Microreactors for Reaction Automation: New Approaches to Reaction Development. *Annu Rev Anal Chem* **2010,** *3*, 19-42.
87. Comer, E.; Organ, M. G., A microreactor for microwave-assisted capillary (continuous flow) organic synthesis. *J Am Chem Soc* **2005,** *127* (22), 8160-8167.
88. Mozharov, S.; Nordon, A.; Littlejohn, D.; Wiles, C.; Watts, P.; Dallin, P.; Girkin, J. M., Improved Method for Kinetic Studies in Microreactors Using Flow Manipulation and Noninvasive Raman Spectrometry. *J Am Chem Soc* **2011,** *133* (10), 3601-3608.

89. Polyzos, A.; O'Brien, M.; Petersen, T. P.; Baxendale, I. R.; Ley, S. V., The Continuous-Flow Synthesis of Carboxylic Acids using CO2 in a Tube-In-Tube Gas Permeable Membrane Reactor. *Angew Chem Int Edit* **2011,** *50* (5), 1190-1193.
90. Wegner, J.; Ceylan, S.; Friese, C.; Kirschning, A., Inductively Heated Oxides Inside Microreactors - Facile Oxidations under Flow Conditions. *Eur J Org Chem* **2010,** (23), 4372-4375.
91. Kawanami, H.; Matsushima, K.; Sato, M.; Ikushima, Y., Rapid and highly selective copper-free Sonogashira coupling in high-pressure, high-temperature water in a microfluidic system. *Angew Chem Int Edit* **2007,** *46* (27), 5129-5132.
92. Rasheed, M.; Wirth, T., Intelligent Microflow: Development of Self-Optimizing Reaction Systems. *Angew Chem Int Edit* **2011,** *50* (2), 357-358.
93. Song, H.; Tice, J. D.; Ismagilov, R. F., A microfluidic system for controlling reaction networks in time. *Angew Chem Int Edit* **2003,** *42* (7), 768-772.
94. Schenk, R.; Hessel, V.; Hofmann, C.; Kiss, J.; Lowe, H.; Ziogas, A., Numbering-up of micro devices: a first liquid-flow splitting unit. *Chem Eng J* **2004,** *101* (1-3), 421-429.
95. Wiles, C.; Watts, P., Continuous flow reactors, a tool for the modern synthetic chemist. *Eur J Org Chem* **2008,** (10), 1655-1671.
96. Krylova, S. M.; Okhonin, V.; Evenhuis, C. J.; Krylov, S. N., The Inject-Mix-React-Separate-and-Quantitate (IMReSQ) approach to studying reactions in capillaries. *Trac-Trend Anal Chem* **2009,** *28* (8), 987-1010.
97. West, J.; Becker, M.; Tombrink, S.; Manz, A., Micro total analysis systems: Latest achievements. *Anal Chem* **2008,** *80* (12), 4403-4419.
98. Hardt, S.; Schönfeld, F., *Microfluidic technologies for miniaturized analysis systems*. Springer: New York, 2007.
99. Okamoto, H.; Ushijima, T.; Kitoh, O., New methods for increasing productivity by using microreactors of planar pumping and alternating pumping types. *Chem Eng J* **2004,** *101* (1-3), 57-63.
100. Kirner, T.; Albert, J.; Gunther, M.; Mayer, G.; Reinhackel, K.; Kohler, J. M., Static micromixers for modular chip reactor arrangements in two-step reactions an photochemical activated processes. *Chem Eng J* **2004,** *101* (1-3), 65-74.
101. Krylova, S. M.; Okhonin, V.; Krylov, S. N., Transverse diffusion of laminar flow profiles - a generic method for mixing reactants in capillary microreactor. *J Sep Sci* **2009,** *32* (5-6), 742-756.
102. Aubin, J.; Fletcher, D. F.; Bertrand, J.; Xuereb, C., Characterization of the mixing quality in micromixers. *Chem Eng Technol* **2003,** *26* (12), 1262-1270.
103. Johnson, T. J.; Ross, D.; Locascio, L. E., Rapid microfluidic mixing. *Anal Chem* **2002,** *74* (1), 45-51.
104. Petrov, A. P.; Dodgson, B. J.; Cherney, L. T.; Krylov, S. N., Predictive measure of quality of micromixing. *Chem Commun* **2011,** *47* (27), 7767-7769.
105. Wong, E.; Okhonin, V.; Berezovski, M. V.; Nozaki, T.; Waldmann, H.; Alexandrov, K.; Krylov, S. N., "Inject-Mix-React-Separate-and-Quantitate" (IMReSQ) method for screening enzyme inhibitors. *J Am Chem Soc* **2008,** *130* (36), 11862-11863.
106. Li, J.; Ge, W.; Wang, W.; Yang, N., Focusing on the meso-scales of multi-scale phenomena-In search for a new paradigm in chemical engineering. *Particuology* **2010,** *8* (6), 634-639.

107. Yunusov, D.; So, M.; Shayan, S.; Okhonin, V.; Musheev, M. U.; Berezovski, M. V.; Krylov, S. N., Kinetic capillary electrophoresis-based affinity screening of aptamer clones. *Anal Chim Acta* **2009,** *631* (1), 102-107.
108. Schrofelbauer, B.; Hakata, Y.; Landau, N. R., HIV-1 Vpr function is mediated by interaction with the damage-specific DNA-binding protein DDB1. *P Natl Acad Sci USA* **2007,** *104* (10), 4130-4135.
109. Verma, M.; Rawool, S.; Bhat, P. J.; Venkatesh, K. V., Biological significance of autoregulation through steady state analysis of genetic networks. *Biosystems* **2006,** *84* (1), 39-48.
110. Margeat, E.; Bourdoncle, A.; Margueron, R.; Poujol, N.; Cavailles, V.; Royer, C., Ligands differentially modulate the protein interactions of the human estrogen receptors alpha and beta. *J Mol Biol* **2003,** *326* (1), 77-92.
111. Pavski, V.; Le, X. C., Ultrasensitive protein-DNA binding assays. *Curr Opin Biotech* **2003,** *14* (1), 65-73.
112. Lin, J. J.; Grosskurth, S. E.; Harlan, S. M.; Gustafson-Wagner, E. A.; Wang, Q., Characterization of cis-regulatory elements and transcription factor binding: gel mobility shift assay. *Methods Mol Biol* **2007,** *366*, 183-201.
113. Pollet, J.; Delport, F.; Janssen, K. P.; Jans, K.; Maes, G.; Pfeiffer, H.; Wevers, M.; Lammertyn, J., Fiber optic SPR biosensing of DNA hybridization and DNA-protein interactions. *Biosens Bioelectron* **2009,** *25* (4), 864-9.
114. Lohman, T. M.; Ferrari, M. E., Escherichia-Coli Single-Stranded DNA-Binding Protein - Multiple DNA-Binding Modes and Cooperativities. *Annu Rev Biochem* **1994,** *63*, 527-570.
115. Wolberg, J. R., *Data analysis using the method of least squares : extracting the most information from experiments*. Springer: Berlin ; New York, 2006; p xiii, 250 p.
116. Molineux, I. J.; Friedman, S.; Gefter, M. L., Purification and Properties of Escherichia-Coli Deoxyribonucleic Acid Unwinding Protein - Effects on Deoxyribonucleic-Acid Synthesis Invitro. *Journal of Biological Chemistry* **1974,** *249* (19), 6090-6098.
117. Cox, M. M.; Lehman, I. R., Reca Protein-Promoted DNA Strand Exchange - Stable Complexes of Reca Protein and Single-Stranded-DNA Formed in the Presence of Atp and Single-Stranded-DNA Binding-Protein. *Journal of Biological Chemistry* **1982,** *257* (14), 8523-8532.
118. Ryzhikov, M.; Koroleva, O.; Postnov, D.; Tran, A.; Korolev, S., Mechanism of RecO recruitment to DNA by single-stranded DNA binding protein. *Nucleic Acids Res* **2011,** *39* (14), 6305-6314.
119. Bujalowski, W.; Lohman, T. M., Escherichia-Coli Single-Strand Binding-Protein Forms Multiple, Distinct Complexes with Single-Stranded-DNA. *Biochemistry-Us* **1986,** *25* (24), 7799-7802.
120. Bujalowski, W.; Overman, L. B.; Lohman, T. M., Binding Mode Transitions of Escherichia-Coli Single-Strand Binding Protein-Single-Stranded DNA Complexes - Cation, Anion, Ph, and Binding Density Effects. *Journal of Biological Chemistry* **1988,** *263* (10), 4629-4640.
121. Ferrari, M. E.; Lohman, T. M., Apparent heat capacity change accompanying a nonspecific protein-DNA interaction. Escherichia coli SSB tetramer binding to oligodeoxyadenylates. *Biochemistry-Us* **1994,** *33* (43), 12896-910.